ILMATIETEEN LAITOS
METEOROLOGISKA INSTITUTET
FINNISH METEOROLOGICAL INSTITUTE

Remote Sensing of Sea Ice

Juha Karvonen et al.

EUMETRAIN/CAL/SAT Marine Course 2013,
November 12, 2013.

Remote Sensing of Sea ice – Some Concepts and Definitions

- The best instruments for sea ice remote sensing are radiometers and SAR's operating at wavelenghts penetrating the cloud cover. Solar illumination is not needed either.
- Optical/IR instruments require cloud masking. Optical instruments additionally require daytime (solar illumination). Also some atmospheric corrections may be required.
- Passive and Active remote sensing.
- VNIR (visible/near-infrared, about 400–1400nm), Mid-IR (about 1.3 to 3 μm), TIR (thermal infrared, 3-30 μm).
- Microwaves: 0.3GHz (1m) to 300GHz (1mm).
- The most important electromagnetic properties: reflection and emission.
- Emission can be expressed by the emissivity coefficient (dimensionsionless) which can be computed from the complex dielectric constant.
- Microwave emission is not as strongly tied to the temperature of an object (as infrared) and more dependent on the object's physical properties.
- The dielectric constant with the target surface roughness determines the emissivity.

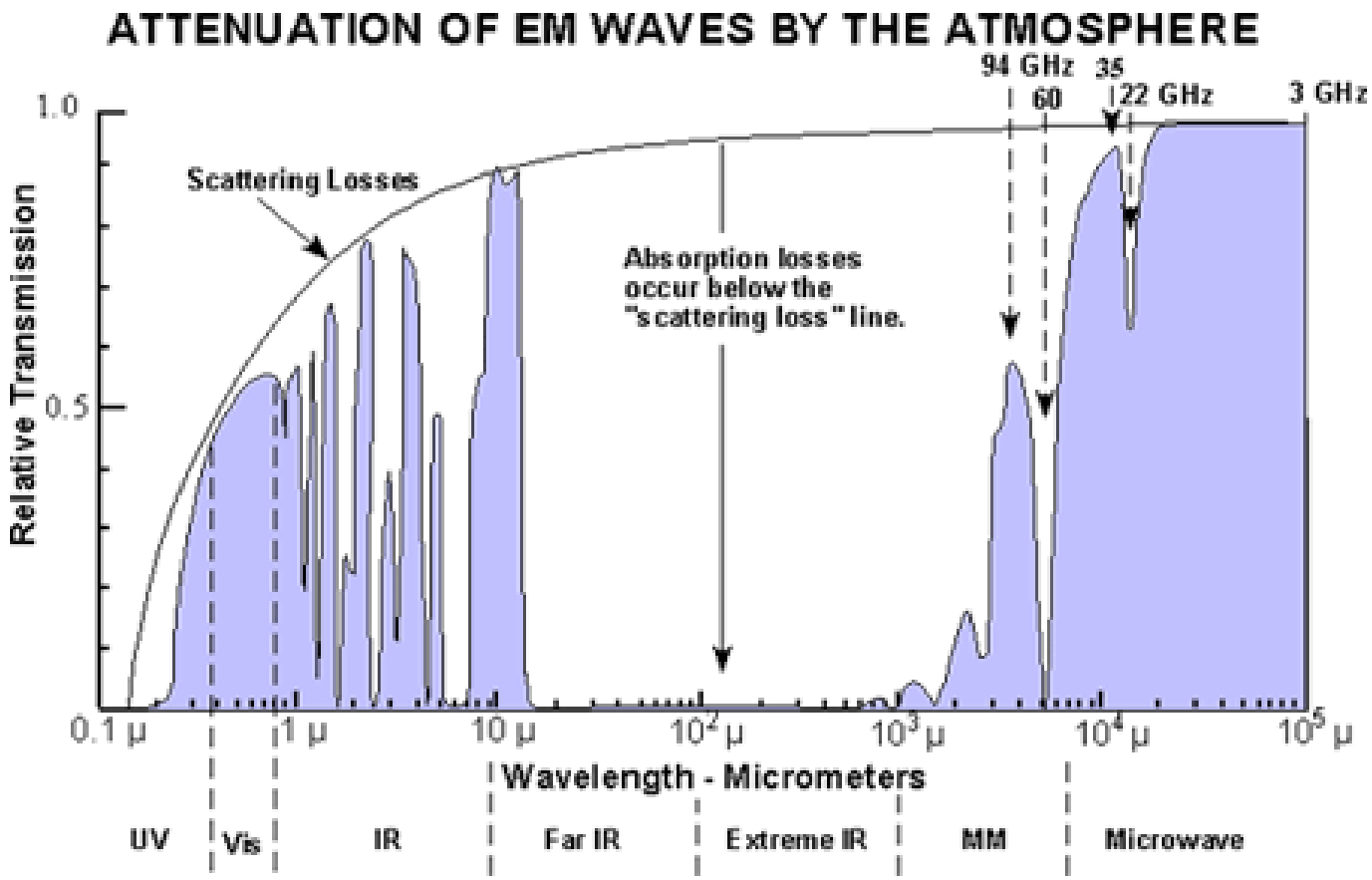

Atmospheric transmission. (Source: www.carboncalculator.co.uk)

- Water is dark at the visible wavelengths and almost a black body at IR wavelenghts.
- This means that water emits thermal radiation with a continuous spectrum that depends on the water temperature.
- The electrical features of material are described by the dielectric constant, ϵ_c, for each medium:

$$\epsilon_c = \epsilon' - i\epsilon''. \tag{1}$$

- The real part ϵ' is the permittivity and the imaginary part ϵ'' is the dielectric loss of the medium.
- Permittivity describes how easily energy passes across the dielectric interface, and the loss term describes how much energy is absorbed in the volume while passing through the dielectric interface.
- For freshwater ice the dielectric constant ϵ' varies only a little as a function of the frequency.
- For saline first-year ice ϵ' is higher and depends on temperature and salinity.
- For sea ice ϵ' is relative constant for frequencies over 1MHz.
- ϵ'' increases as the function of the salt content of the ice, e.g. multiyear ice has lower ϵ'' than first-year ice.

- Passive microwave instruments can be used for sea ice concentration retrieval.
- The radiative transfer equation is the basis for algorithms to get geophysical parameters from the measured data.
- Brightness temperature (T_b) = the temperature of the black body which radiates the same radiant energy as an observed object. If the object is a black body, then the real temperature is equal to the brightness temperature.
- The brightness temperature, measured by an instrument can be divided into four terms: signal from the earth surface, atmospheric upwelling, atmospheric downwelling, and cosmic background component.

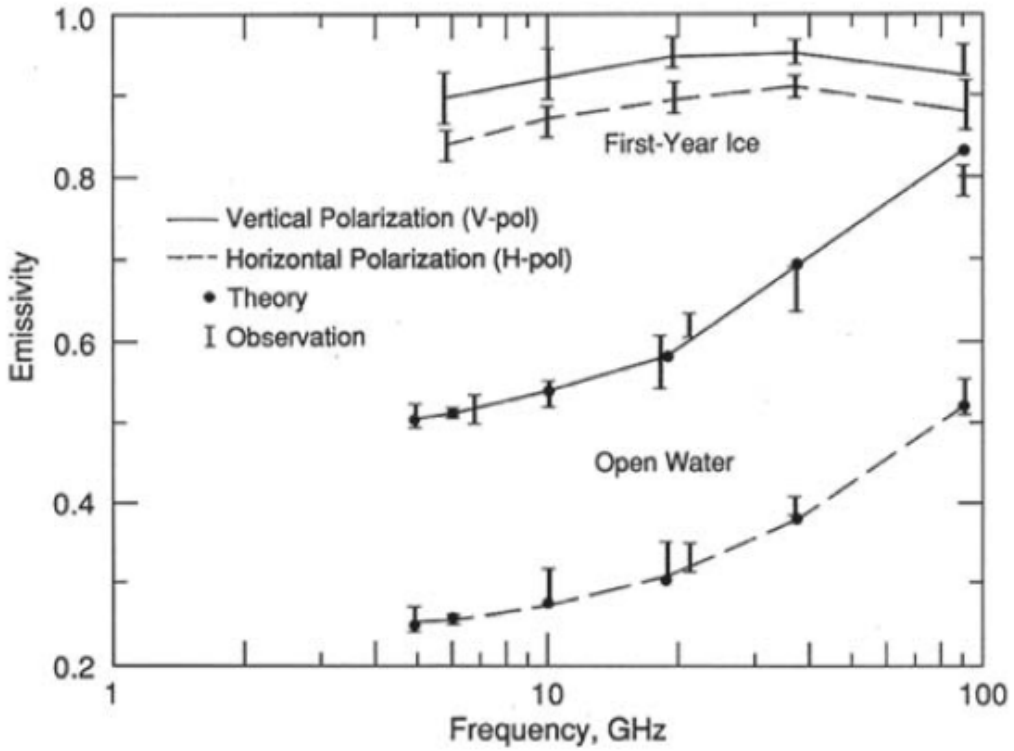

Theoretical and observed emissivities for first-year ice and calm water, for both vertical and horizontal polarization as a function of frequency (Source: Carsey, Microwave remote sensing of sea ice, American Geophysical Union, 1992).

- Passive microwave radiometers measure the emitted MW radiation in multiple channels and polarizations. The measured quantity is the brightness temperature:
  $T_b = T_s(\epsilon(\lambda))^{1/4}$,
  T_s is the target surface temperature and ϵ is the emissivity. If ϵ is independent of λ then the object is a gray body. For a black body $\epsilon(\lambda) = 1$.
- Large foorprints.
- Basic idea to estimate ice concentration: a measurement is a linear combination of the ice and water components with different MW signatures.
- Multi-frequency algorithms applied to estimate the ice concentration, e.g. the NASA team algorithm using a difference between two channels normalized by their sum. This reduces the affect of the temperature.
- Ice surface temperature can be estimates using IR $\rightarrow$ thin ice thickness in cold conditions can be retrieved (the thicker the ice the colder ST), the value saturates at about 50-100 cm (ice acts as an insulator for the water heat).

Thin ice thickness estimation (Yu and Rothrock, JGR, v. 101, C11, pp. 25753-25766, 1996)

- Requires cloud recognition, applied only for the clear sky data.
- Equation of energy conservation at the top surface (snow(on ice)/air interface):

$$(1.0 - \alpha_s)F_r - l_0 - F_l^{up} + F_l^{dwn} + F_s + F_e + F_c = 0$$

α_s surface albedo, derived from visible channels of the EO instrument

F_r incoming solar radiation, estimated emprically (for clear sky condition), dependent on solar zenith angle and surface water vapour pressure

l_0 radiation passing through the interior, estimated a function of the thickness of the snow and ice

F_l^{up} upward longwave radiation, derived from the surface temperature by the EO instrument

F_l^{dwn} downward longwave radiation, empirical estimation, requires the near-surface (2m) air temperature

F_s turbulent sensible heat flux (i.e. flux related to changing temperature), estimated based on the wind, surface and air temperatures, bulk transfer coefficients for heat and evaporation

F_e latent heat flux (i.e. flux related constant temperature processes), estimated based on the wind, surface and air temperatures, bulk transfer coefficients for heat and evaporation

F_c conductive heat flux (in the presence of temperature gradients), linear temperature gradients in snow/ice can be assumed: $F_c = \gamma(T_f - T_s)$, T_f is the seawater freezing temperature. γ is dependent on the ice and snow thickness (H_i and H_s)

- During dark seasons we can drop the first two terms:
  $-F_l^{up} + F_l^{dwn} + F_s + F_e + F_c = 0$

- The snow thickness H_s is unknown, different empirical parametrizations to present H_s as a function of H_i have been proposed. The best solution would be to extract H_s from EO data.
- After defining H_s or its dependency on H_i, H_i appearing in the conductive heat flux term F_c can be solved.
- This methodology has been applied to AVHRR (Advanced Very High Resolution Radiometer, a NOAA instrument with 5 visible/IR channels), and MODIS (Moderate-Resolution Imaging Spectroradiometer, a NASA instrument with 36 visible/IR channels).
- Requires cold, cloudless conditions. Only thin ice estimation possible due to saturation for higher ice thickness values.

Thin ice thickness detection based on AMSR-E and AMSR-2

- Advanced Microwave Scanning Radiometer-EOS (AMSR-E) and AMSR-2 with 36.5 and 89 GHz channels.
- Thin ice up to 10-20cm (Tamura and Oshima, JGR, v. 116, C07030, 2011).
- Linear or exponential mapping between polarization ratio (V/H) and ice thickness.
- Thin ice emission properties mainly depend on the near surface salinity, which decreases with increasing ice thickness, i.e. this is indirect estimation.
- PSSM (polynya signature simulation method, Hunewinkel et al., TGRS, n. 36, v. 5, 1795-1808, 1998) classified radiometer data to OW, FYI, thin ice (or low concentration ice), can not distinguish between low concentration with thickner ice and thin ice.
- Spectral difference = brightness temperature difference
- Spectral gradient = brightness temperature difference divided by frequency difference
- Radiometer polarization ratios and spectral gradient ratios have been studied at FMI for Arctic thin ice thickness detection.
- Large uncertainty only two categories of thin ice (<20cm) and thicker ice.

Altimetry

- Altimeter measures the distance to the ice/sea surface $\rightarrow$ freeboard (here denoted by E) $\rightarrow$ ice thickness by the Archimedes principle.
- Requires some approximation of the snow/ice cover density.
- Basic equation, assuming only ice with a constant density $H_i = \frac{E\rho w}{\rho w - \rho_i}$, in practice snow on ice must be taken into account, leading to estimation of the snow thickness and density and relatively large uncertainty.
- In practice altimeter resolutions are too sparse for e,g, the Baltic Sea.
- ICESat and ICESat-II (NASA), LIDAR altimeter. ICESat operation ended in Feb 2010, ICESAT-II sheduled to be launched in 2015.
- CryoSat's (ESA) primary instrument is SIRAL (SAR / Interferometric Radar Altimeter).
- SIRAL has three modes:
  - Traditional altimeter mode.
  - SAR mode (i.e. coherently transmitted echoes are combined to reduce the footprint).
  - Interferometric SAR mode. Utilizing the second antenna of the instrument.
- Typically low areal and vertical resolution.

SAR Marine Applications

- Wind
  - Based on SAR backscattering from water (Bragg scatering)
  - Theoretically known wind speed and magnitude relative to the satellite track can be converted to a σ^0 value, but the inverse is not possible.
- Waves
  - Wave spectrum from SAR data (by local 2-D FFT)
  - Restricted by SAR resolution, e.g. in the Baltic Sea typical wavelenghts can not be seen.
- Ships and other objects with strong backscattering (e.g. icebergs)
  - Locating bright targets with respect to the background and analysing their ignatures (shape, brightness)
- Oil slick, algae, other possible thin films
  - Based on the attenuation effect of a thin film on the water, i.e. these areas appear darker in SAR.
  - Restricted by the waves (require some waves to attenuate, but not too large)

- Sea ice
- Storms, atmospheric vertices (larger scale patterns in SAR)
- Rainfall (attenuation at higher frequencies, e.g. at X-band)
- etc...

SAR

- SAR (Synthetic Aperture Radar) is an active air- or spaceborne instrument transmitting and receiving EM radiation at (around) a certain frequency.
- Sensitive to surface roughness unlike MW instruments.
- Advantages of SAR compared to (most) passive RS instruments:
  - Does not need solar illumination, works well in nighttime also (very important in sea ice remote sensing because in the winter there is no daylight in the north).
  - Typical SAR frequencies penetrate the cloud cover, typically no atmosphere correction is needed.
  - In many cases can also give information on the target inner structure (volume scattering) in addition to the surface (surface scattering).

- In the azimuth direction (instrument flight direction) the same location is measured multiple times at a slightly different frequency (because of the different relative velocity with respect to the target, at different locations of the instrument, i.e. Doppler effect).
- The range resolution is improved by using a chirp pulse (increasing frequency) $\rightarrow$ the information is spread and pulse compression is needed.
- The same technique (pulse compression) in both range and azimuth directions, e.g. using a matched filter to get the final SAR image.
- Moving targets cause problems in the azimuth signal compression, because their motion is unknown to the SAR processor and the relative speed depends on both the target and the platform motions.

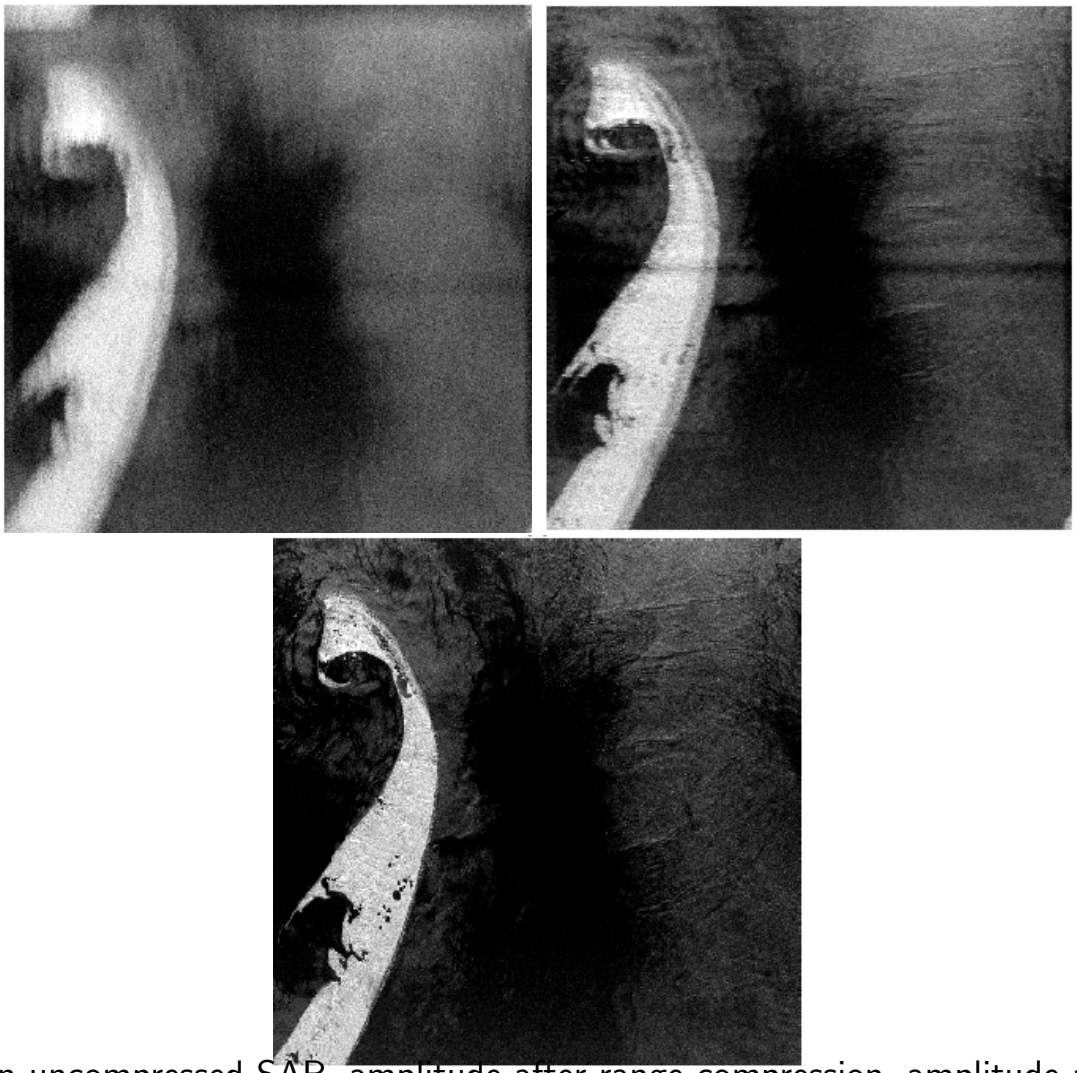

Amplitude of an uncompressed SAR, amplitude after range compression, amplitude after range and azimuth compression.

Band	λ (mm)	f (GHz)
Ka	8–11	40–26.5
K	11–17	26.5–18
Ku	17–24	18–12.5
X	24–38	12.5–8
C	38–75	8–4
S	75–150	4–2
L	150–300	2–1
P	300–1000	1–0.3

Typical radar frequency bands.

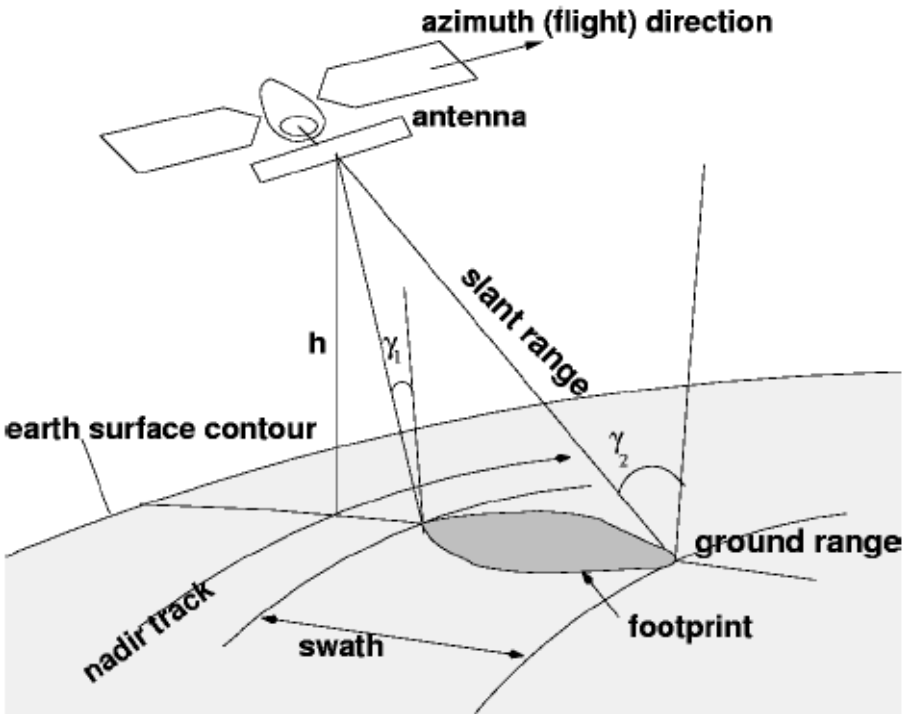

SAR imaging geometry.

- Radar cross section (RCS, denoted by σ_R) is a property of a single target, describing how well the target reflects the radar energy. RCS is the energy received by the sensor relative to the energy received in the case of an isotropic (i.e. scattering equal to all directions) scatterer.
- The backscattering coefficient, σ^0, is the average scattering cross section per unit area
  $\sigma^0 = E[\frac{\sigma_i}{A_i}]$
  where σ_i and A_i describe the RCS and area of a single scatterer inside the resolution cell (image pixel), and E is the expectation operator. Backscattering coefficient is a normalized version of the radar cross section, describing the backscatter properties of a pixel area, probably containing several different backscatterers.
- The backscattering coefficient is usually expressed in logarithmic scale and in decibels (dB): ${\sigma^0}_{\mathrm{dB}} = 10 \log_{10} \sigma^0$.
- For the isotropic case ${\sigma^0}_{\mathrm{dB}} = 0$ dB. If the scattering is focused toward the receiving antenna then ${\sigma^0}_{\mathrm{dB}} > 0$ dB, and if the scattering is focused away from the receiving antenna then ${\sigma^0}_{\mathrm{dB}} < 0$ dB. Typically a very high backscattering, e.g. from urban areas or very rough surfaces is higher than $-5dB$, and high backscatter from rough surfaces (e.g. dense vegetation) is between $-10dB$ and $0dB$. Smooth surfaces (e.g. calm water or level ice) produce low backscatter, typically below $-20dB$.

- The relation between the transmitted and received power (for a single point scatterer) is defined by the radar equation
  $P_r = \frac{P_t {G_A}^2 \lambda^2}{(4\pi)^3 R^4} \sigma,$
  where σ is the RCS, P_r is the received power, P_t is the transmitted power, G_A is the antenna power gain, λ is the wavelength and R is the distance to the object.
- This can be divided into a radar characteristics part ($P_t G^2 \lambda^2$) and a target characteristics part ($\frac{\sigma}{R^4}$).
- For a distributed target (area), it is an integral over the area:
  $P_r = \frac{\lambda^2}{(4\pi)^3} \int \frac{P_t G^2 \sigma^0}{R^4} dA$
  (this is relative to R^2 instead of R^4)

- The measured SAR intensity is:
  $I_{\mathrm{SAR}} = \sigma_{\mathrm{R}} n,$
  where n is a noise term, also known as speckle. The received and averaged intensity is K-distributed.
- σ^0 can be computed based on the measured SAR intensity I or amplitude A:

$$\sigma^0 = \frac{A^2}{K}\sin(\alpha) = \frac{I}{K}\sin(\alpha), \tag{2}$$

- K is a calibration coefficient defined for a SAR instrument defined based on targets with known properties (e.g. corner reflectors).
- Typically σ^0 is given in dB:

$$\sigma^0(dB) = 10log_{10}(\sigma^0). \tag{3}$$

- SAR interferometry: Phase difference of two simultaneous measurements or measurements with a short time gap at the same location from different platform locations $\rightarrow$ interference patterns can be used to get altitude contours.
- Phase unwrapping algorithms to convert the intereference data into surface elevation models.
- Ice surface structure for static ice can be measured if there is a time gap between the measurements. If there is no time gap, ice surface structure can be obtained for moving ice also.
- SAR polarimetry. Four polarimetric channels (HH, HV; VH, VV).
- SAR tomography: the altitude of the backscattering by means of SAR interferometry using fully polarimetric data and using multiple orbits (measurements) from different angles, interferometric polarimetry. Suitable for e.g. remote sensing of forests (tree parameters).
- Current operational SAR-instruments typically produce either one polarization (HH) or two polarizations (HH/HV). Fully polarimetric data is only available over small areas.
- Compact polarimetry SAR's in the future: emulates polarimetric SAR by transmitting circularly polarized (or 45 degrees polarization) signal and receiving H and V polarizations (RISAT-1 and Radarsat constellation).

Basic Steps of SAR Processing

1. SAR processor $\rightarrow$ Georeferenced SAR image.
2. Georectification $\rightarrow$ Geocoded SAR image in a desired projection and resolution (resampling).
3. Image preprocessing
   - Calibration
   - Incidence angle correction
   - Speckle reduction
   - Contrast enhancement
   - ...
4. Image interpretation (automated or visual) $\rightarrow$ user products
5. Validation of the results

SAR and Snow

- At C and X bands some snow volume scattering occurs if the snow is not dry. At longer wavelengths (S, L, P bands) the effect of snow is smaller.
- C-band SAR still penetrates dry snow well, thus dry snow has practically no effect on the measurement.
- Wet snow is a problem. The SAR backscattering is attenuated by the wet snow layer.
- Typically snow has not been taken into account in sea ice SAR algorithms (dry snow assumption), or different parameters are used for wet and dry snow.
- Snow on sea ice difficult to estimate. Some estimates can be made by inversion of emission modeling of radiometer data (e.g. AMSR).
- Snow on sea ice needs different parametrization than snow on land.

Operational Space-Borne SAR Instruments

- Sun synchronous polar orbit (i.e. passing through or close to poles, and ascending or descending approximately at the same time over the same location).
- Typically at about 700-800 km height.
- ALOS-PALSAR (Japan, L-band), until April 21, 2011.
- PALSAR-2 (Japan, L-band)
- ENVISAT ASAR (ESA, C-band), until April 8, 2012.
- RADARSAT-1 (Canada, C-band), ScanSAR mode, HH, resolution about 100m, until March 29, 2013.
- RADARSAT-2 (Canada, C-band), ScanSAR mode, HH/HV, resolution about 100m.
- COSMO-SkyMed (Italy, X-band), HR mode HH (200km x 200km) , resolution 100m, a constellation of four satellites.
- TerraSAR-X and TenDEM-X (Germany, X-band, two satellites), ScanSAR (200km) available from 09/2013.
- RISAT-1 (C-band, India) and RISAT-2 (X-band).

- Chinese environmental SAR satellite HJ-1-C (S-band), not working.
- Sentinel-1 (ESA, C-band, two satellites, first in 2014), HH/HV in ScanSAR mode.
- RADARSAT-constellation (Canada, C-band, three satellites), 2018.

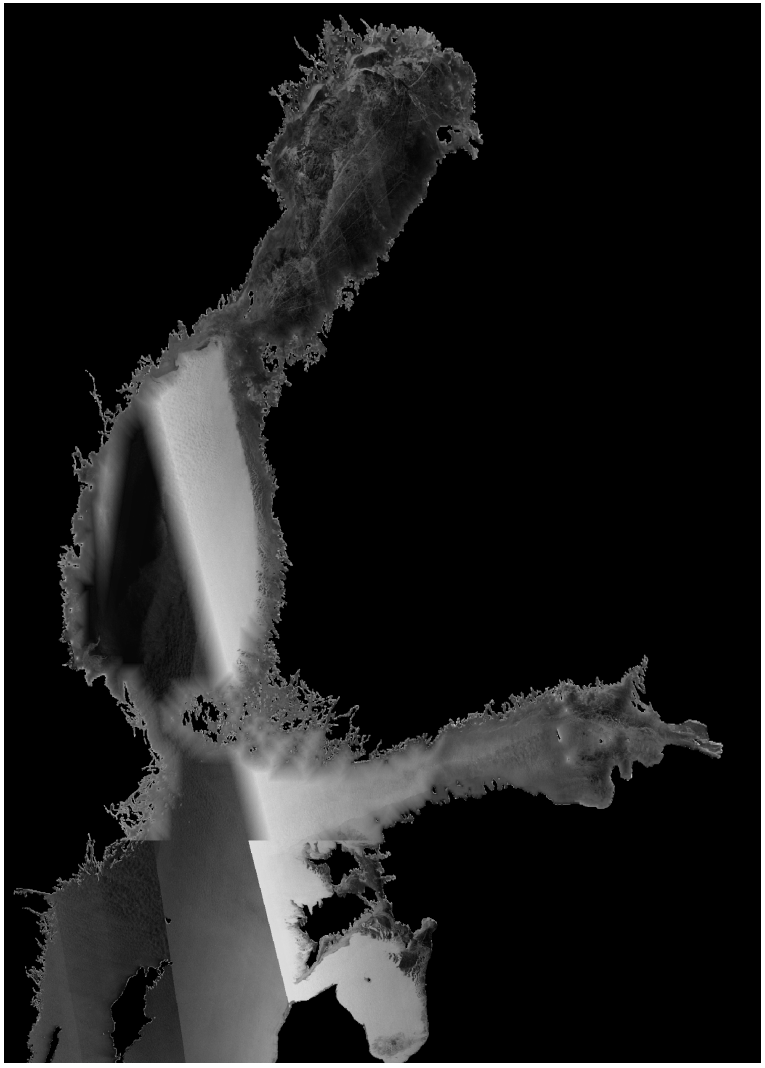

SAR mosaic over the Baltic Sea, Feb 1, 2012.

ILMATIETEEN LAITOS
METEOROLOGISKA INSTITUTET
FINNISH METEOROLOGICAL INSTITUTE

Visual recognition of sea ice in SAR

- Open water: close to Gaussian noise, σ^0 varies a lot depending on the wave spectrum.
- Young thin ice: typically dark (low σ^0, reflecting away from the instrument)
- Deformed ice: σ^0 typically increases as a function of the ice deformation.
- Details (ridges, leads, ship tracks, brash ice barriers etc...): recognized based on shape and location.

- Also automated products like ice thickness charts and ice motion estimates are produced operationally (polarview and MyOcean products).
- Sea ice classes/parameters
  - Age: first-year, second-year, multi-year.
  - Large scale structure: level ice, deformed ice (rafted ice, ridged ice).
  - Ice thickness.
  - Ice concentration (%) $C = 100 \times A_i/A$.
- In the Baltic Sea only first year ice, in the Arctic areas also second-year ice and multi-year ice (more than two years old) exist.
- Rough sea ice classification: open water, level ice (thin in the Baltic), deformed ice and highly deformed ice, fast ice. These classes can be identified by SAR rather well.
- Currently either HH only or HH/HV combination used. The advantages of using fully polarimetric data have been studied.

- Simple sea ice classes detectable by SAR
  - Open water
  - Level ice
  - Deformed Ice
  - Highly Deformed Ice
  - Fast Ice
  - Second year and multiyear ice (in Arctic)

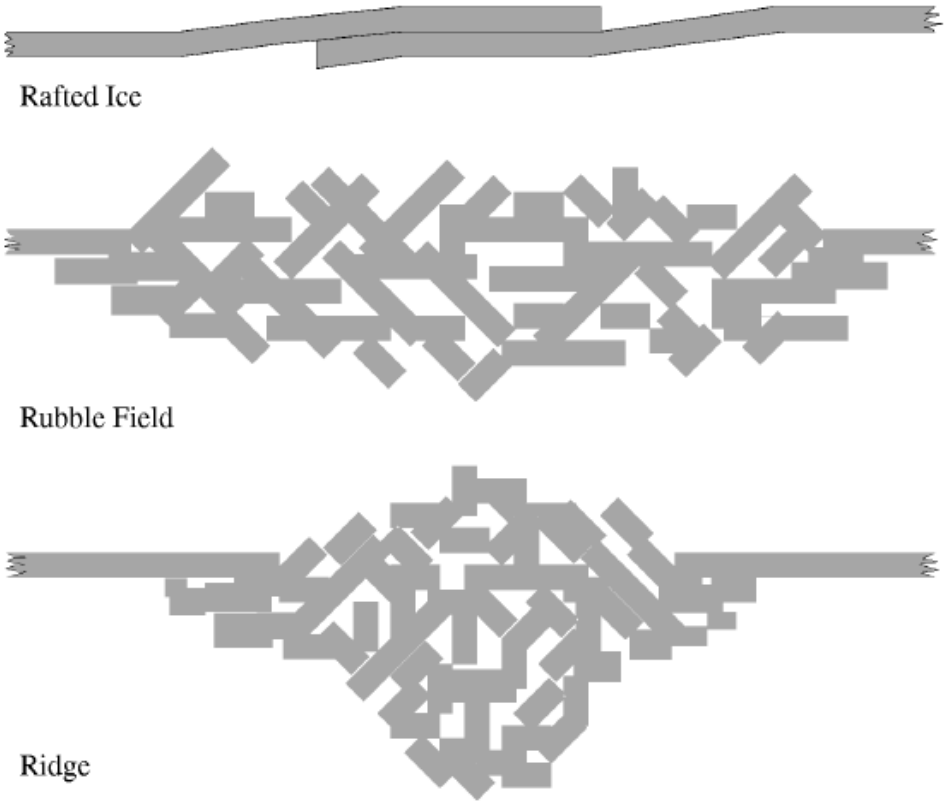

Forms of deformed ice. The SAR backscattering from rubble fields and ridges is typically higher than from rafted ice, and even less from level ice.

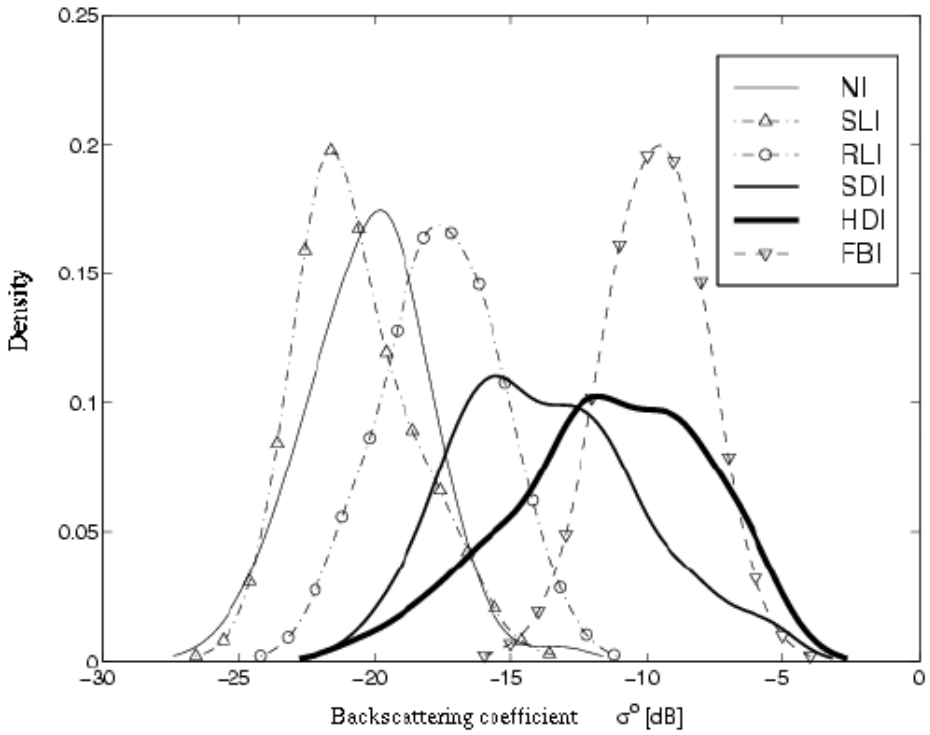

Backscattering (σ^0)distributions for different ice types at incidence angle of 23 degrees (©Marko Makynen, FMI).

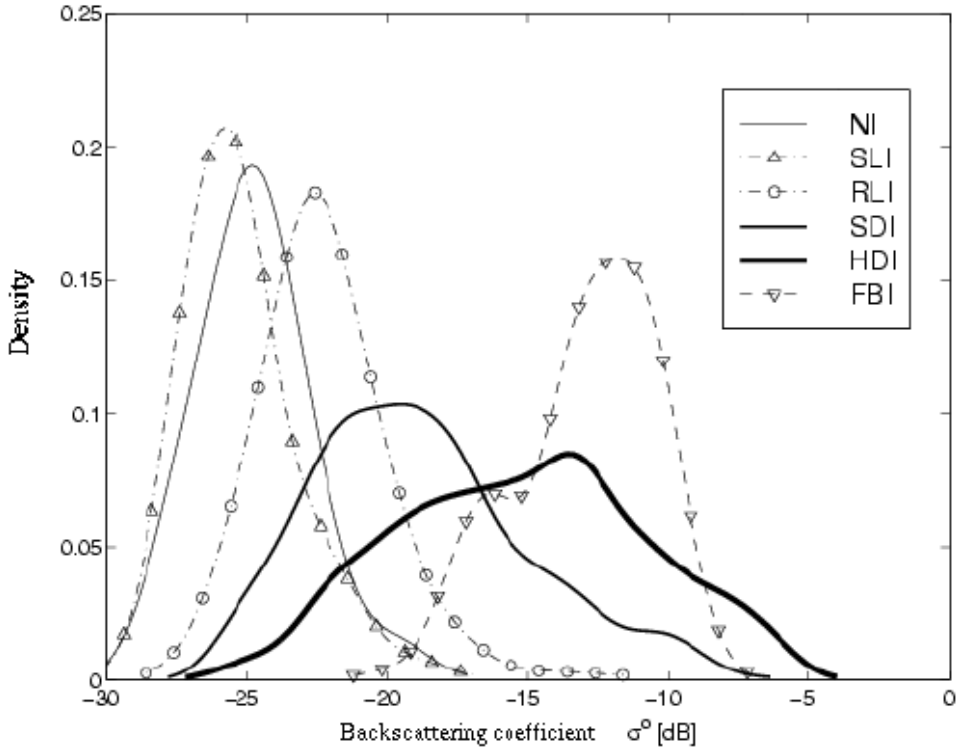

Backscattering (σ^0)distributions for different ice types at incidence angle of 45 degrees (©Marko Makynen, FMI).

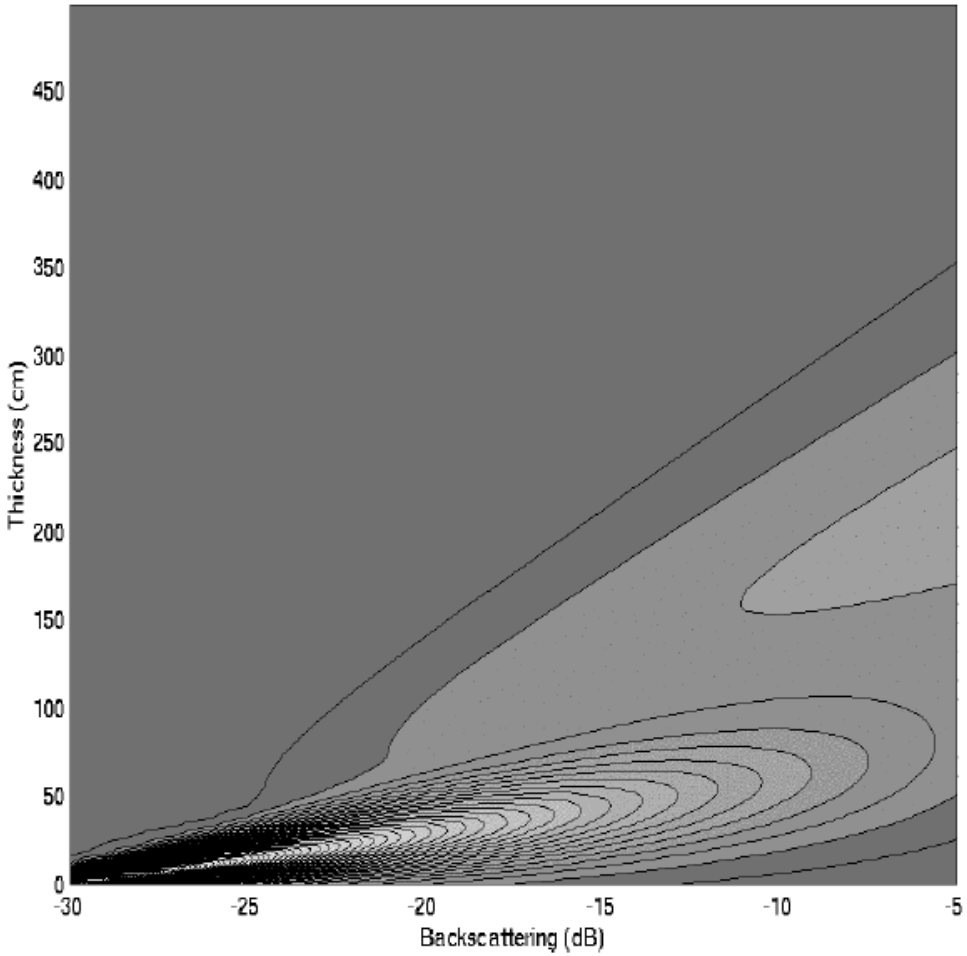

Statistical dependence of ice thickness and SAR backscattering coefficient for the Baltic Sea ice.

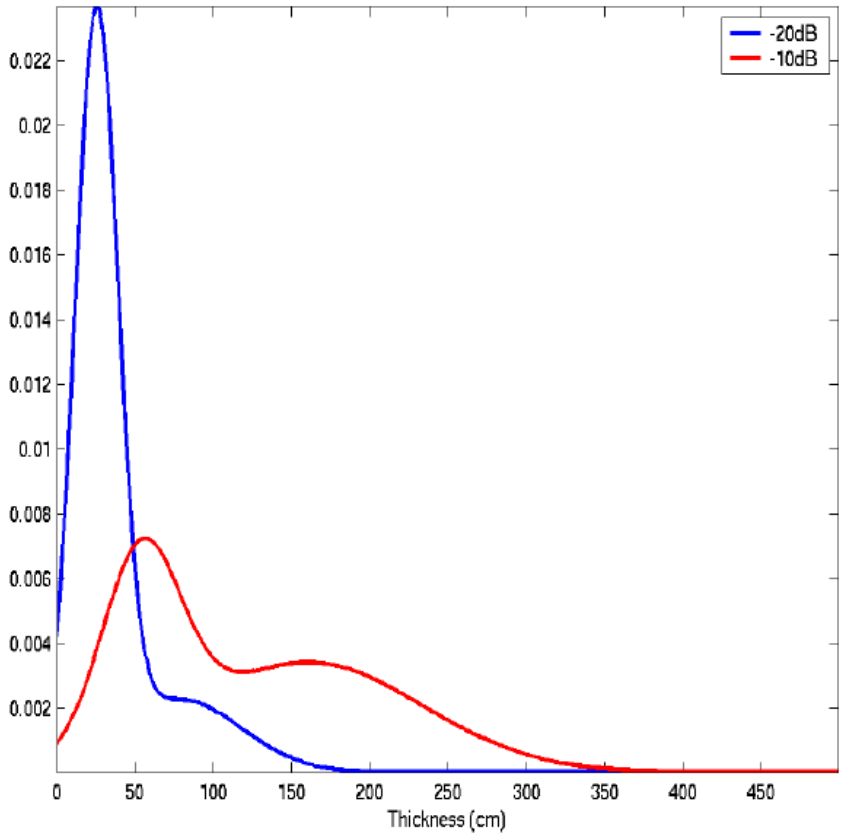

Statistical dependence of ice thickness and SAR backscattering coefficient for the Baltic Sea ice, at -10dB and -20dB.

Georectification

- Mercator projection in the Baltic Sea (used in nautical charts).
- In the polar areas polar stereographic or Lambert conformal conic projection.
- gdal-library routines (like gdal-translate and gdalwarp) used for the rectification (utilizes the proj4 library).
- Typical SAR output resolution 100m.

SAR Segmentation

- Some SAR Segmentation Methods:
  - ICM (Iterated conditional modes). Relatively fast, automated parameter initialization possible.
  - MRF based on simulated annealing. Slow, automated parameter initialization possible.
  - Pulse-Coupled Neural Network (PCNN) for intensity (incidence angle corrected σ^0) segmentation. Relatively fast, automated definition of the parameters difficult.
  - K-means or isodata segmentation with two features (intensity and local autocorrelation). Fast, required an initial value for K.

Segmentation Based on Markov Random Fields

- Goal is to find an optimal labeling L in condition of having measured features f, i.e. the MAP estimate would be
  $\hat{L}_{MAP} = argmax_{L \in \Omega} P(L|f)$
- According to the Bayes theorem
  $P(L|f) = \frac{P(f|L)P(L)}{P(f)} \propto P(f|L)P(L)$
  (P(f) is a constant).
- Hammerley-Clifford theorem: for an MRF P(L) is Gibbs distributed i.e.:
  $P(L) = \frac{1}{Z} exp(-U(L)) = \frac{1}{Z} exp(-\sum_{c \in C} V_c(L))$,
  where $Z = \sum_{L \in \Omega} exp(-U(L))$, $U(L)$ is the energy function, $V_c(L)$ is a clique potential (cliques are sets of neighboring pixels).
- The labels (classes) are presented by Gaussian distributions i.e.
  $P(f_s|L_s) = \frac{1}{\sqrt{2\pi}\sigma_{L_s}} \exp \frac{(f_s - \mu_{L_s})^2}{2\sigma^2_{L_s}}$

- Favoring similar pixels in the (simple) neighborhood: $V_{C_2} = \beta\delta(L_i, L_j)$, $\delta(L_i, L_j) = 1$ if $L_i = L_j$, and -1 otherwise. For larger cliques (neighborhoods) V_c's become more complex.
- Then the (log) energy is
  $U(L) = \sum_S (\log((2\pi)^{1/2}\sigma_{Ls}) + \frac{(f_s - \mu_{Ls})^2}{2\sigma_{Ls}^2} + \sum_{s,r} \beta\delta(w_s, w_r)$
- $P(L|f) = \frac{1}{Z}\exp(-U(L)) \rightarrow \hat{L}_{MAP}$=argmax$_L$ P(L|f) = argmin$_L$ U(L)
- Approaches to minimize the energy function $U(L)$:
  - Gradient descent (can get stuck in a local minimum)
  - Simulated annealing (Metropolis), the labeling is dependent on the temperature, if the energy function U(L) value increases, the label is changed with a probability dependent on the temperature and increase of U(L) ($\exp(-\Delta U/T)$)
- Computation time consuming. However, a MRF segmantation can be computed for a 500m resolution image in a few minutes on a desktop PC.

An example of a SAR image (Feb 13, 2013, Bay of Bothnia), and MRF segmentation with the segments filled with the segment mean values.

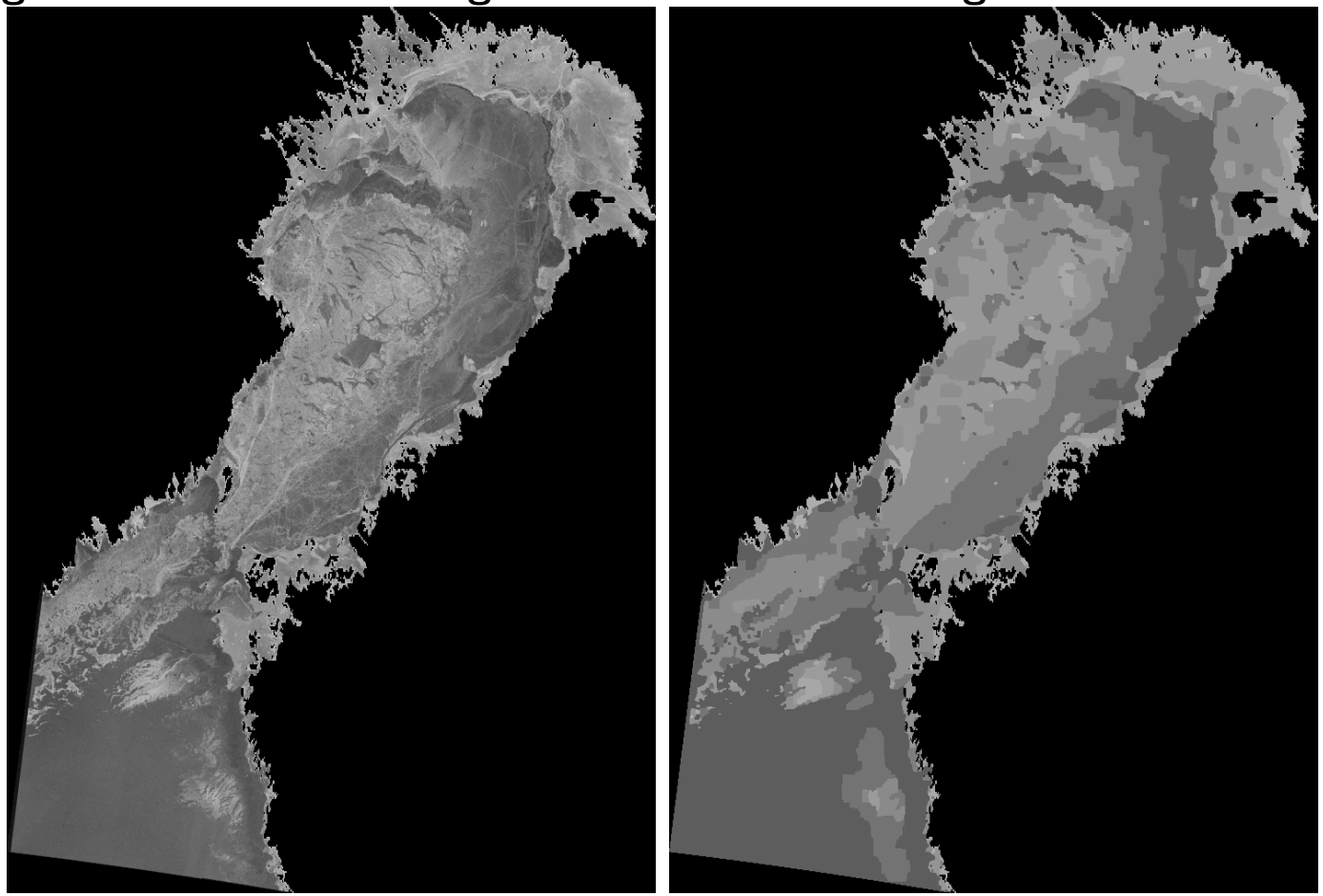

Edge Detection

- Canny edge detection algorithm.
- Based on gradient magnitude and hysteresis (dual) thresholding.
- Also Harris edge and corner detection algorithm has been studied. Corners could give additional local information on the complexity of the sea ice structure.
- Edges can be divided into random and structured edges based on the edge segment size. Structured edges can be assumed to represent some real structures in the SAR images, and random edges are assumed to include the noise.

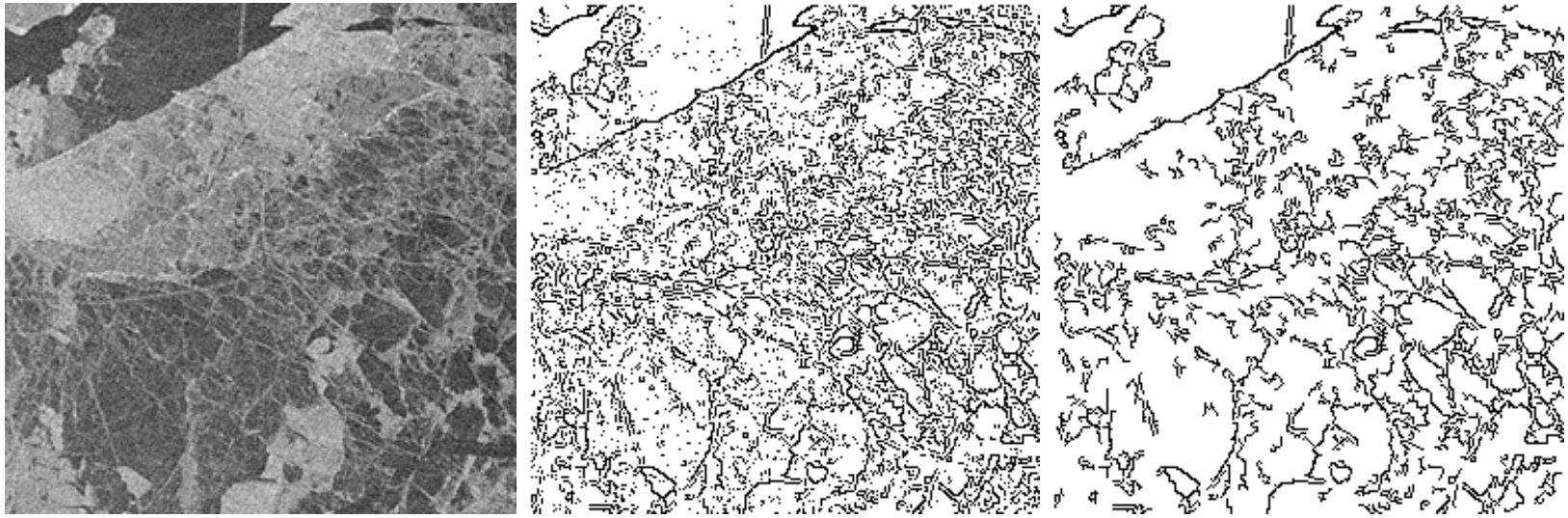

A part of a SAR image ($\approx$ 25x25 km, left), detected edges (middle) and the corresponding structured edges (i.e. edges which are parts of larger edge segments than a given threshold, here 10, right).

ILMATIETEEN LAITOS
METEOROLOGISKA INSTITUTET
FINNISH METEOROLOGICAL INSTITUTE

Speckle Reduction

- Many methods have been studied for use at FMI.
- In some cases logarithm is applied to SAR data before speckle reduction, this is assumed to make the multiplicative noise present in SAR additive.
- Existing algorithms e.g.
  - Gamma-MAP, based on SAR statistics
  - Median and iterative median
  - Unisotropic diffusion
  - Kuwahara
  - Wavelet-based algorithms, thresholding of the high-frequency coefficients.
  - Lee filtering
  - SNN (symmetric nearest neighbor)
  - ...
- Anisotropic iterative median algorithm used at FMI.
- Iterative 3x3 median, not computed over the detected edges.
- Median applied on one side of an edge (non-edge pixel) or along the edge (edge pixel).

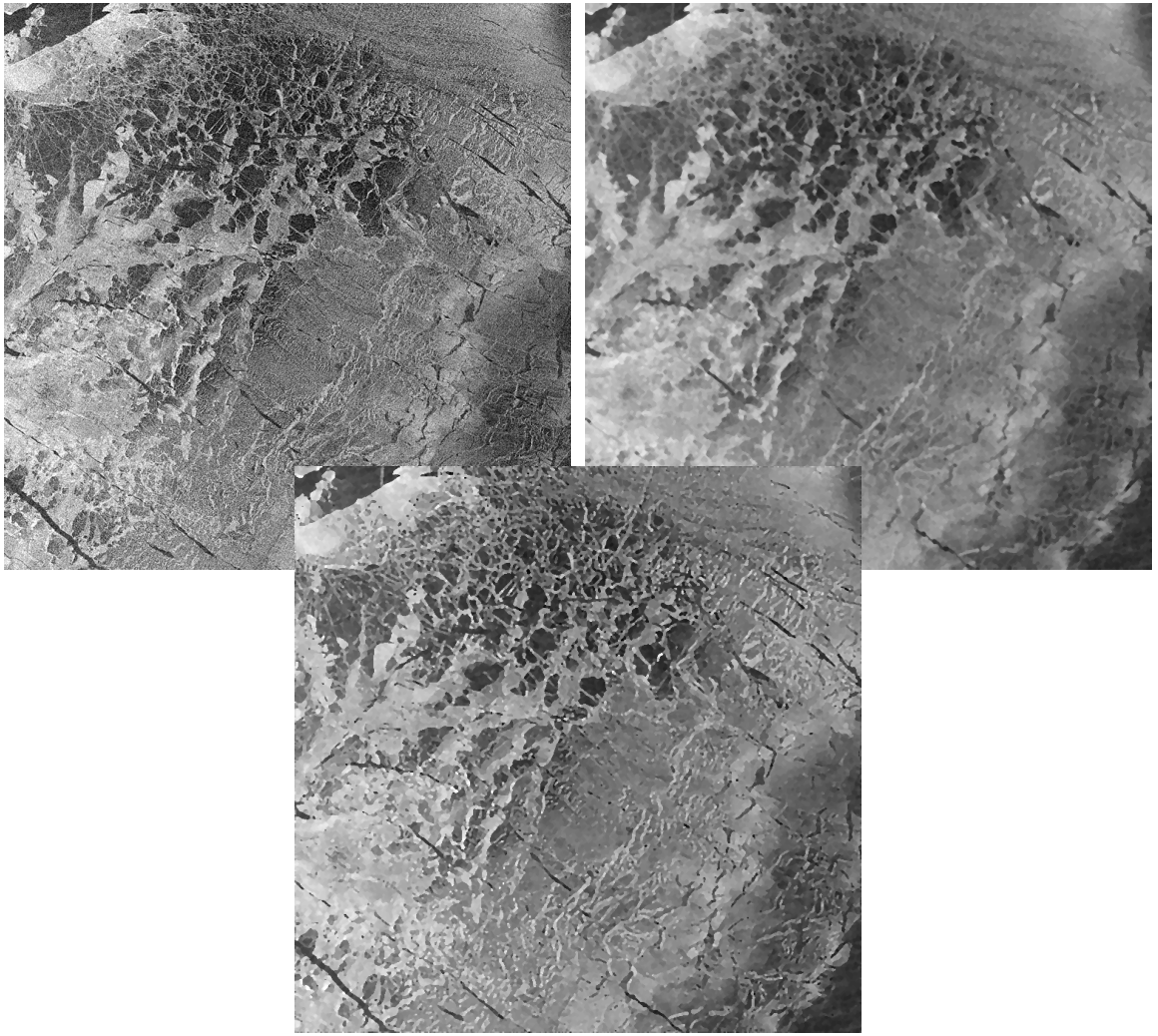

An example of speckle filtering, the original Radarsat-1 image ($\approx$ 75x75 km), iterative 3x3 median (40 iterations) and anisotropic 3x3 median (40 iterations).

ILMATIETEEN LAITOS
METEOROLOGISKA INSTITUTET
FINNISH METEOROLOGICAL INSTITUTE

Incidence Angle Correction

- A linear correction based on large Baltic Sea ice statistics (σ^0 in dB) is computed.
- Different slopes for level ice and deformed ice are applied.
- Division into level ice and deformed ice is made based on the amount of edges.

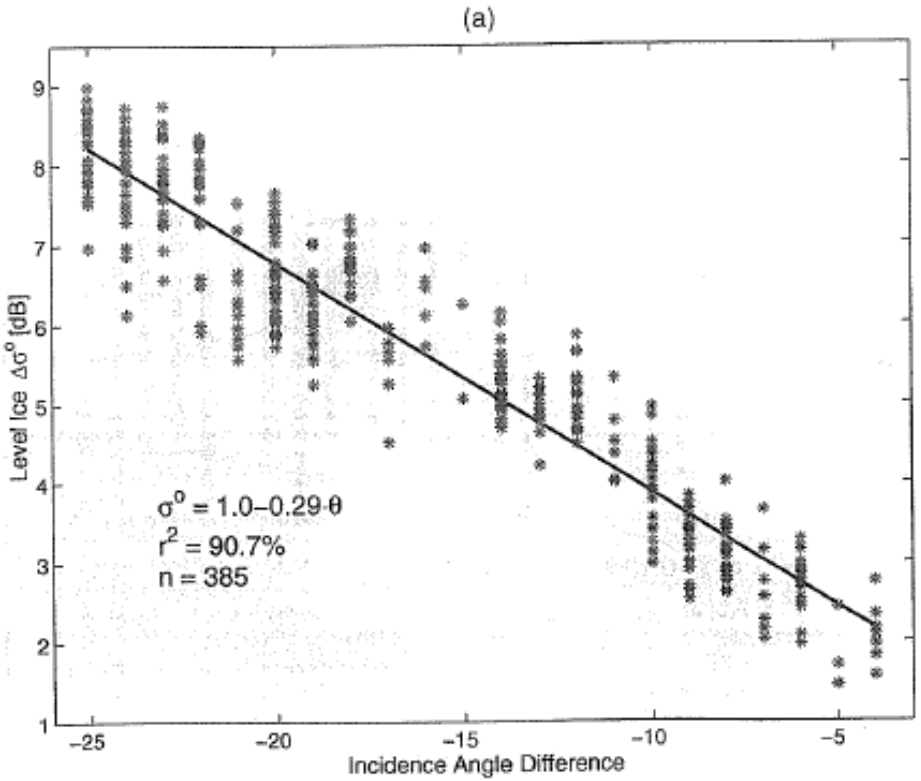

Incidence angle dependence of σ^0 for level ice.

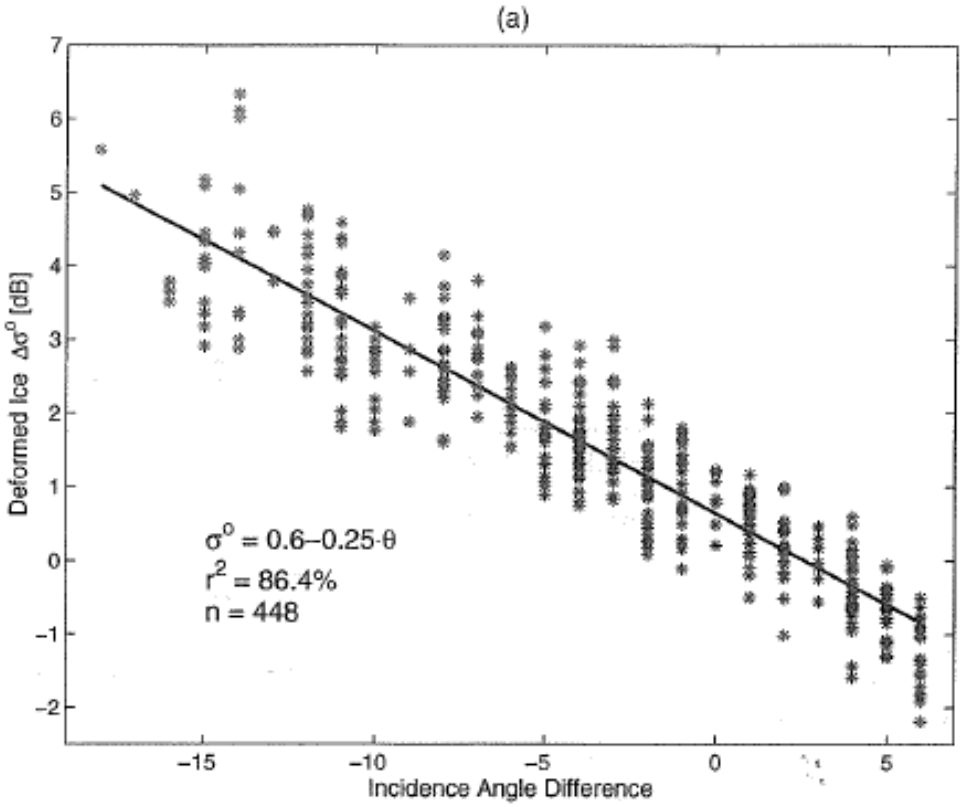

Incidence angle dependence of σ^0 for deformed ice.

Some Texture Features

- Local autocorrelation
  $C(k,l) = \frac{\frac{1}{|B|}\sum_{\mathrm{ij}\in\mathrm{B}}\left(I(i-k,j-l)-\mu_B\right)\left(I(i,j)-\mu_B\right)}{\sigma_B^2},$
- Moments
  $m_1 = \frac{1}{N}\sum_{i=1}^{N} x_i$
  $m_k = \frac{1}{N}\sum_{i=1}^{N}(x_i-\mu)^k$, k=2...
- (Normalized) Kurtosis
  $M_4 = \frac{m_4}{\sigma^4} - 3.$
  Measure of the Gaussianity.
- Moment ratios, e.g. $R_{12} = \frac{m_1^2}{m_2}$ (ENL).
- Local gradient based features.
- Amount of edges and structured edges.

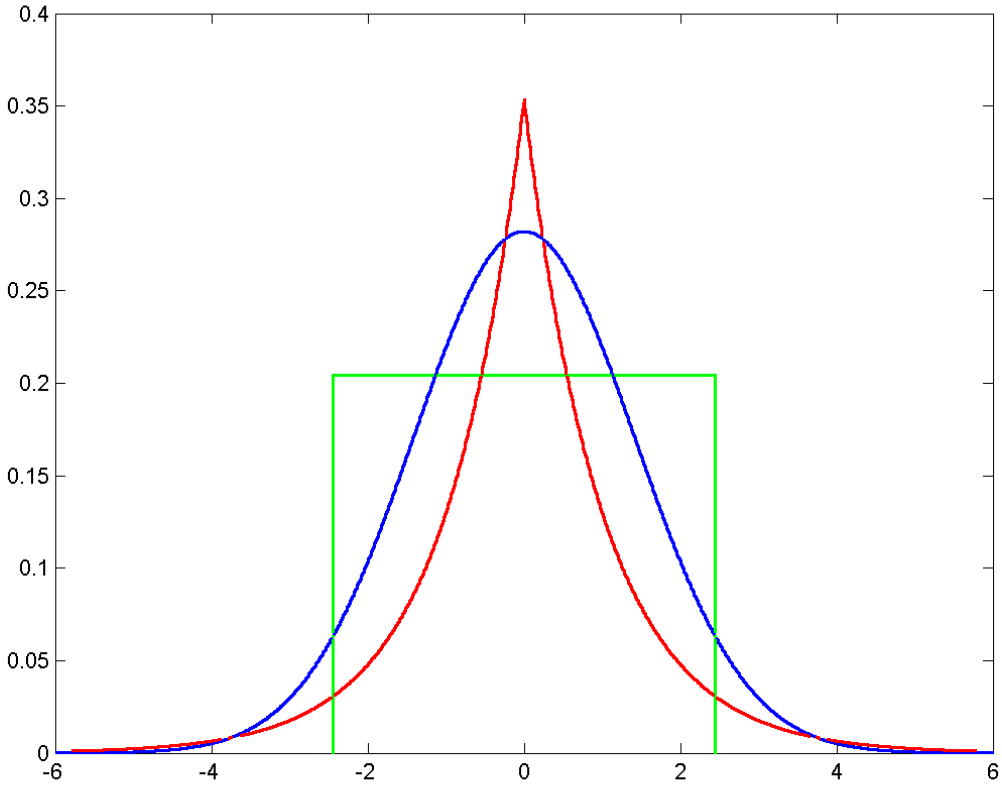

Gaussian distribution ($K = 0$), Laplace distribution (subgaussian i.e. $K < 0$, having higher peak and heavier tails than the gaussian) and uniform distribution (supergaussian, $K > 0$).

Ice Concentration

- Ice concentration: the proportion of the ice covered area over a given area. It is given either in ratio ($0.0 \rightarrow 1.0$) or percentage ($0\% \rightarrow 100\%$).
- Ice concentration is dependent on the scale, in fine enough scale the ice concentration is either zero (open water) or one (ice).
- High-resolution ice concentration information are required for navigation, validating of ice models and data assimilation.
- The currently available operational ice concentration products are based on microwave radiometer data and their resolution is several kilometers. E.g. University of Bremen delivers operational (global) ice concentration products based on AMSR-E data using an algorithm called the ASI algorithm.
- SAR data cover large sea and ocean areas with much higher precision than that of the radiometer data, and they have not been very efficiently utilized in e.g. measuring of ice concentration.

- The AC distribution $p(x)$ for each segment is decomposed into a mixture of M Gaussians $g_k(x)$:
  $p(x) = \sum_{k=1}^{M} \alpha_k g_k(x)$.
  α_k are the weights (proportions) of the M Gaussians and $\sum_{k=1}^{M} \alpha_k = 1.0$.
- For each segment the aucorrelation distribution is computed and these distributions are decomposed into Gaussian mixtures using the Em algorithm.
- The number of Gaussians, M, for each segment is incremented until the maximum allowed number of Gaussians (e.g. 10) is achieved or the coefficient of determination, R^2, between the actual distribution and the mixture of the M Gaussians exceeds a given threshold (e.g. 0.95)

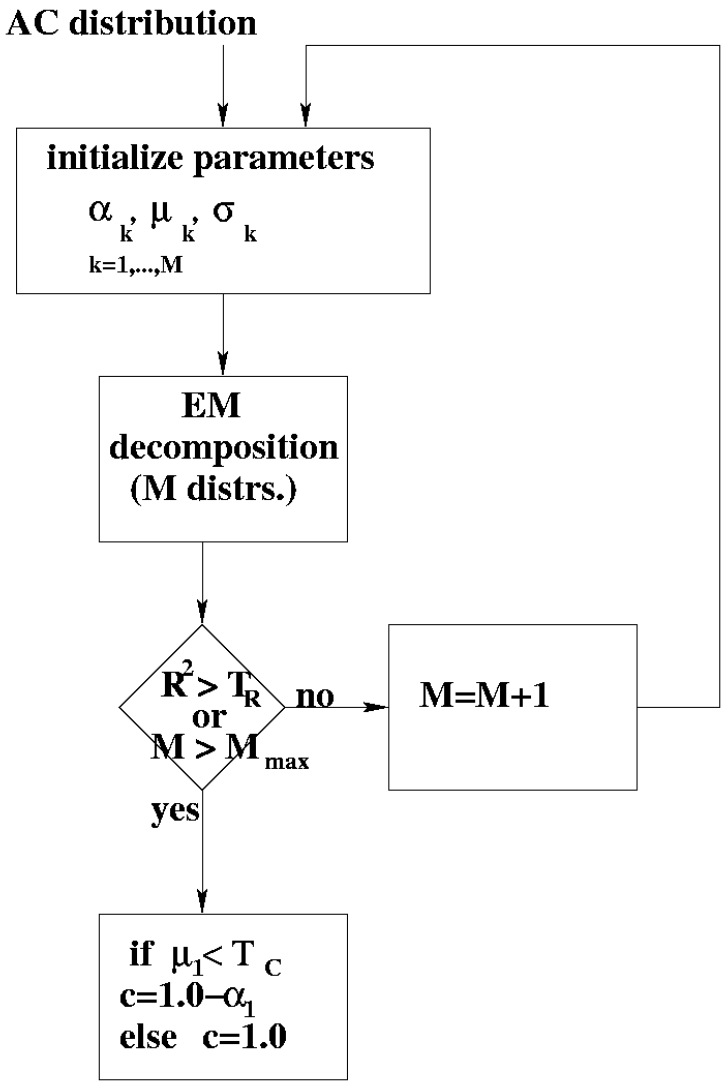

Algorithm for a single segment concentration estimate.

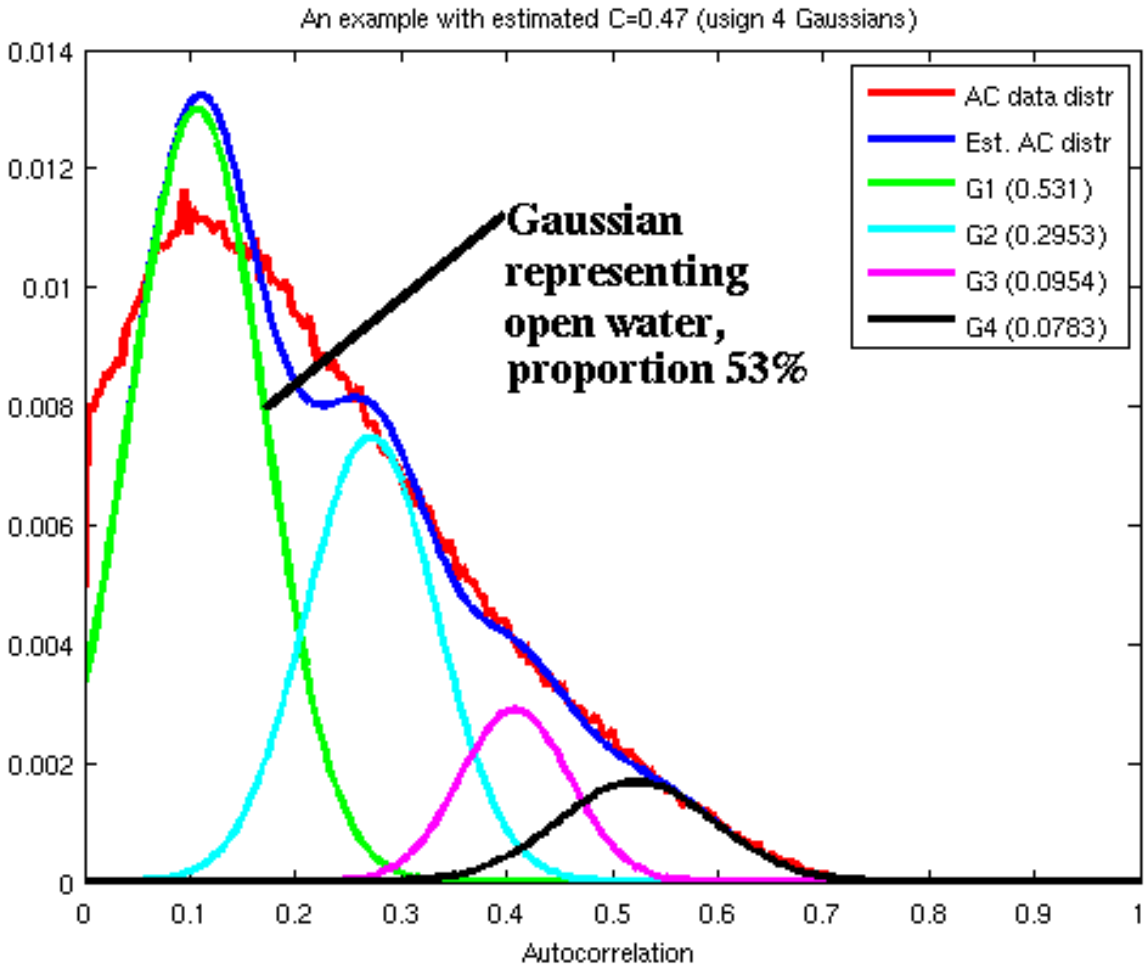

An example of a decomposition into four Gaussians and the corresponding concentration estimate.

- An algorithm for dual-polarized data has also been developed.
- The algorithm is based on a MLP neural network.
- MLP architecture: 6-10-1.
- HH-channel concentration estimate used as one input to the MLP.
- Other inputs: Three HV-related features and the incidence angle (segment means).
- Adaptive learning EBP rate: reduced if the error inreases, otherwise increased.
- Advantages: It is not necessary to model the dependencies (especially the indicence angle dependednce).
- Disadvantages: A black box, dependencies modelled by the MLP.
- The HV channel improves the estimation, compared to FIS ice charts (and the ASI algorithm, based on AMSR-E data). The L_1 error was reduced about 20% compared to the L_1 error for the HH algorithm with fast ice correction. (ASI 21.2%, FMI IC 19.6%).

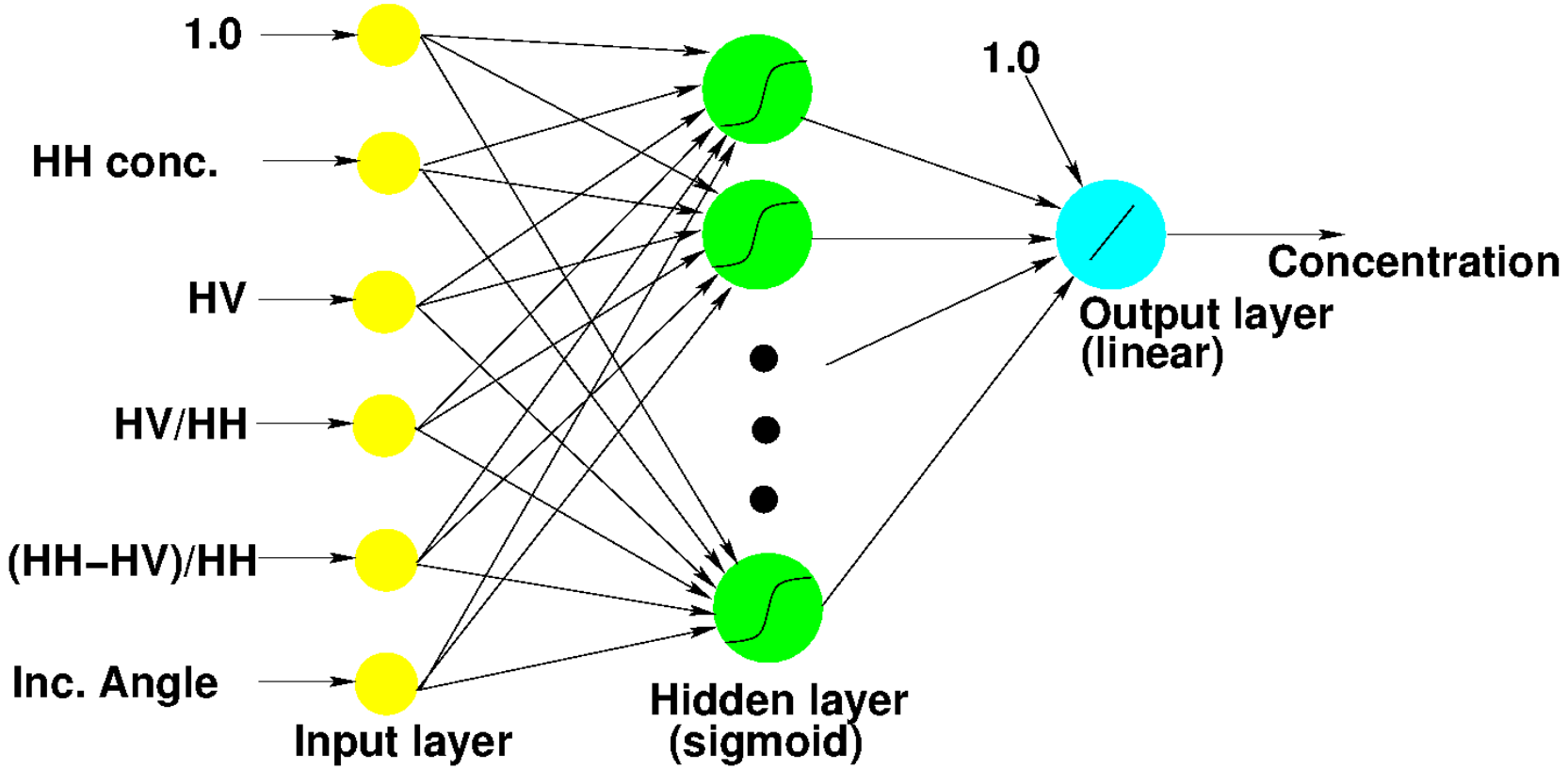

The MLP NN structure.

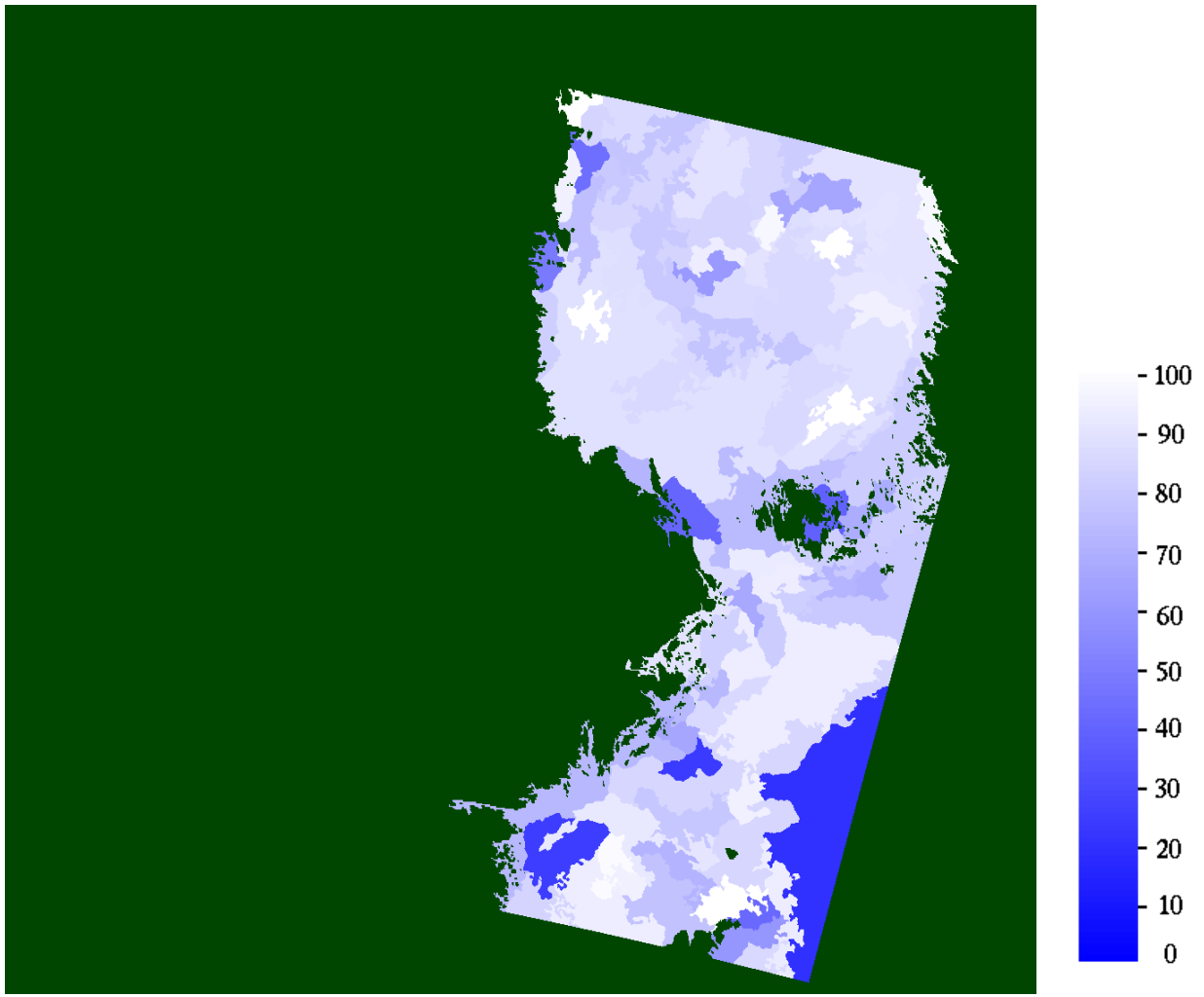

Estimated ice concentration based on HH-channel data March 2 2011 at 05:16:46 UTC.

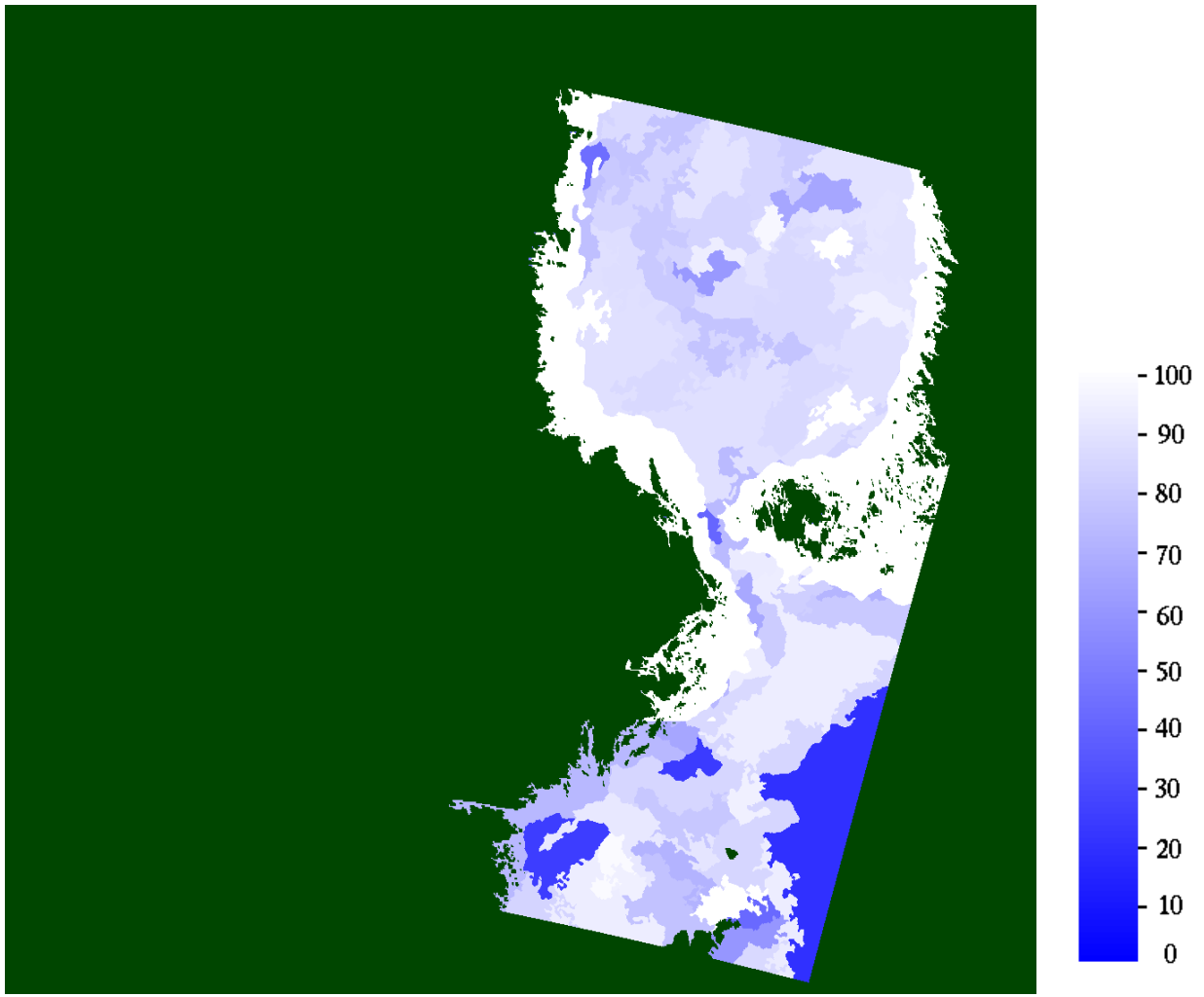

Estimated ice concentration based on HH-channel data with fast ice correction.

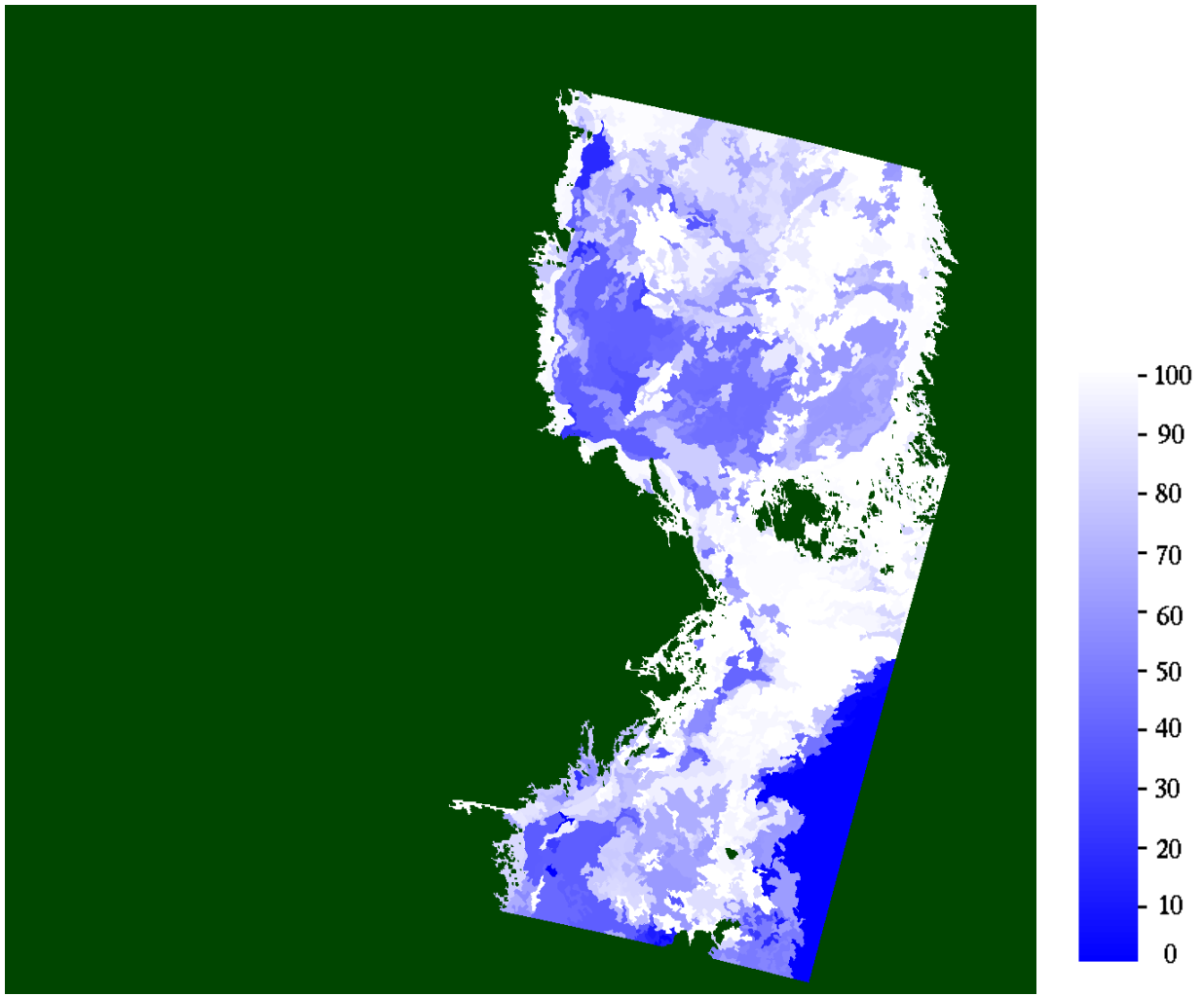

Estimated ice concentration based on HH/HV-channel data.

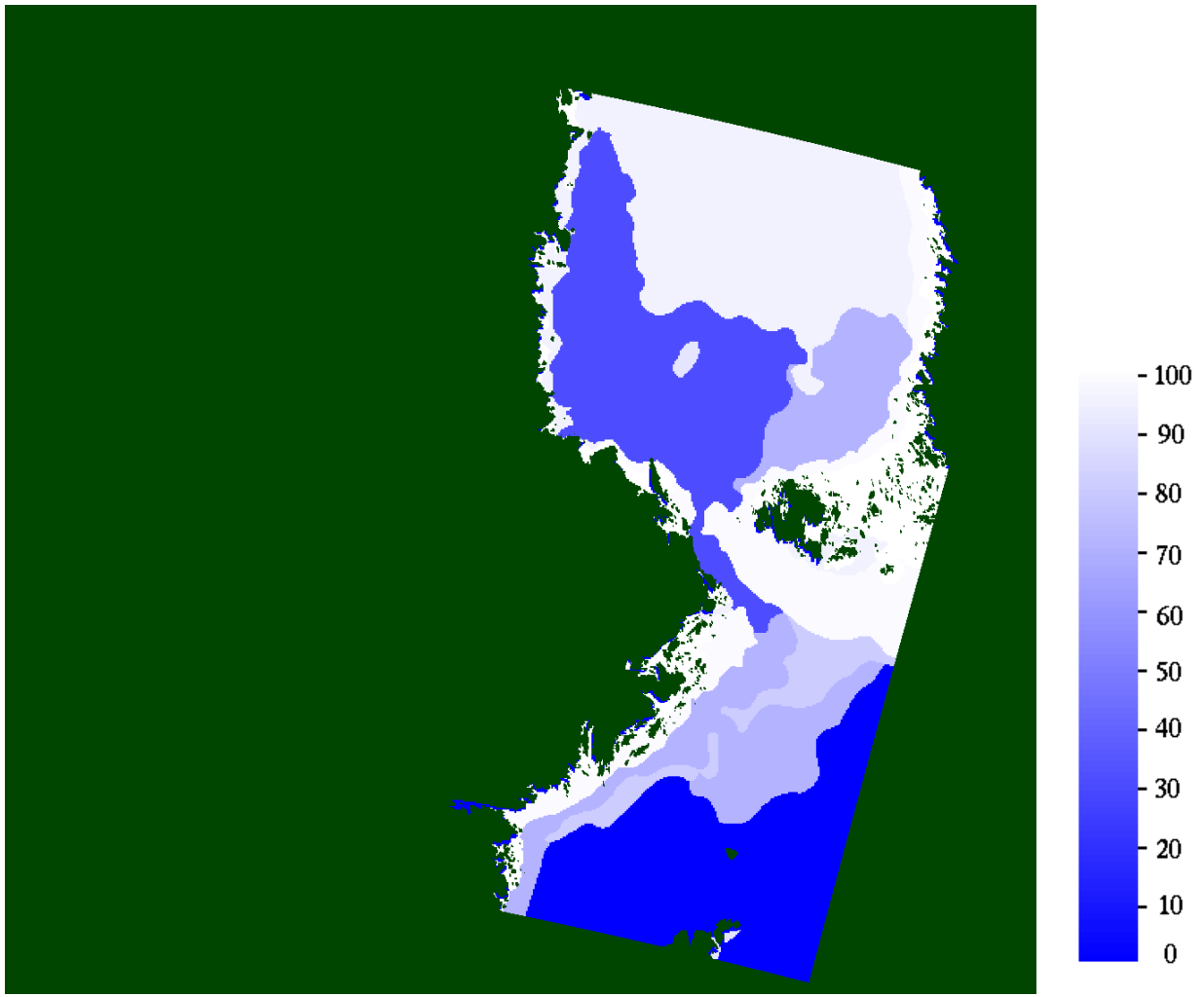

Ice concentration of the FMI ice chart March 2 2011.

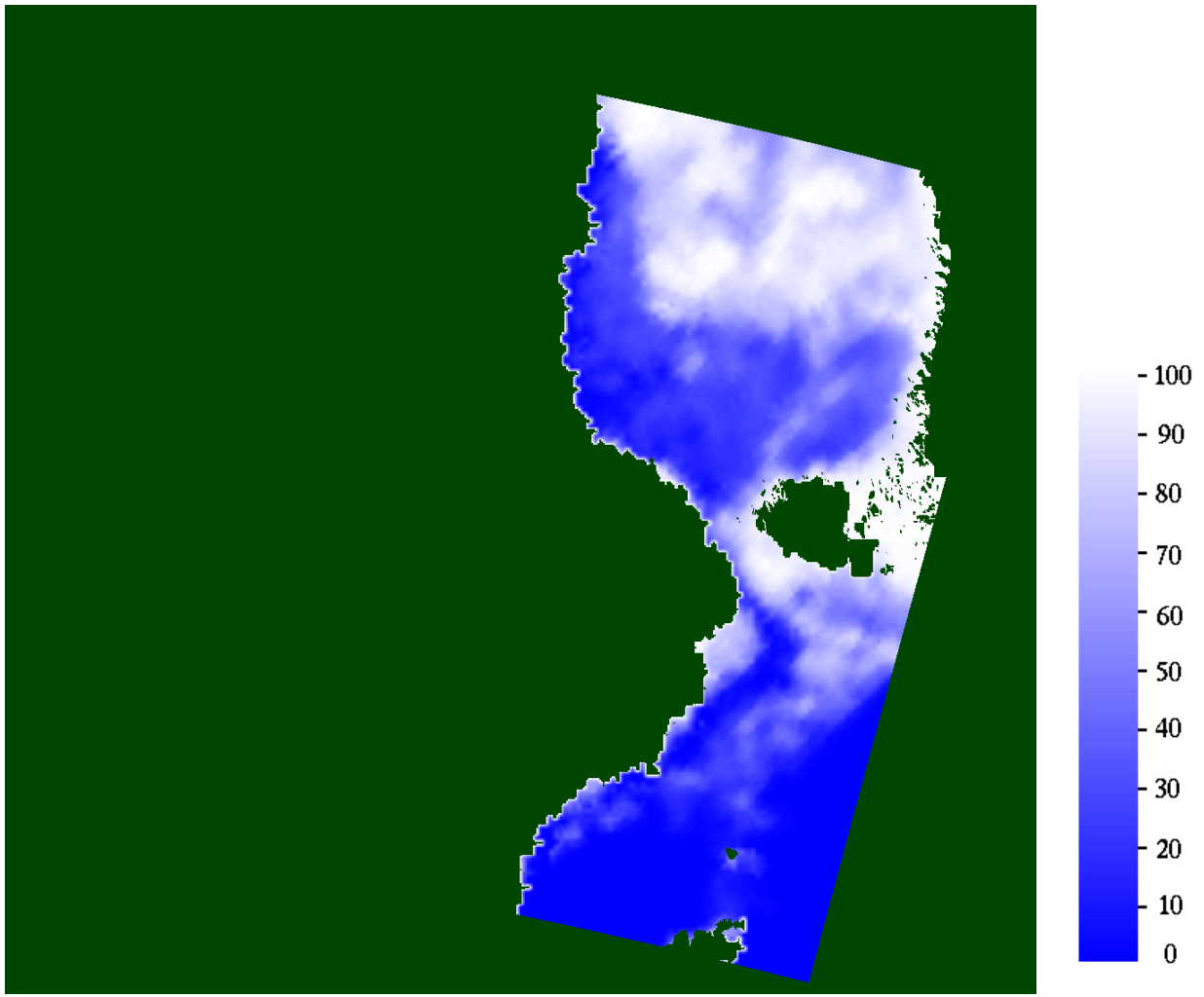

ASI (AMSR-E) ice concentration March 2 2011.

ILMATIETEEN LAITOS
METEOROLOGISKA INSTITUTET
FINNISH METEOROLOGICAL INSTITUTE

Ice Thickness

- The ice thickness history information derived from digitized ice charts is refined based on SAR data.
- Both segment boundaries and the thickness values assigned to segments are refined.
- Run operationally after a SAR image (Radarsat-1 or Envisat ASAR) is received, and the resulting thickness charts are delivered to the ice breakers and also available on the web as thematic charts at **polarview.fimr.fi**.
- Also available in numeric format at **myocean.eu**.

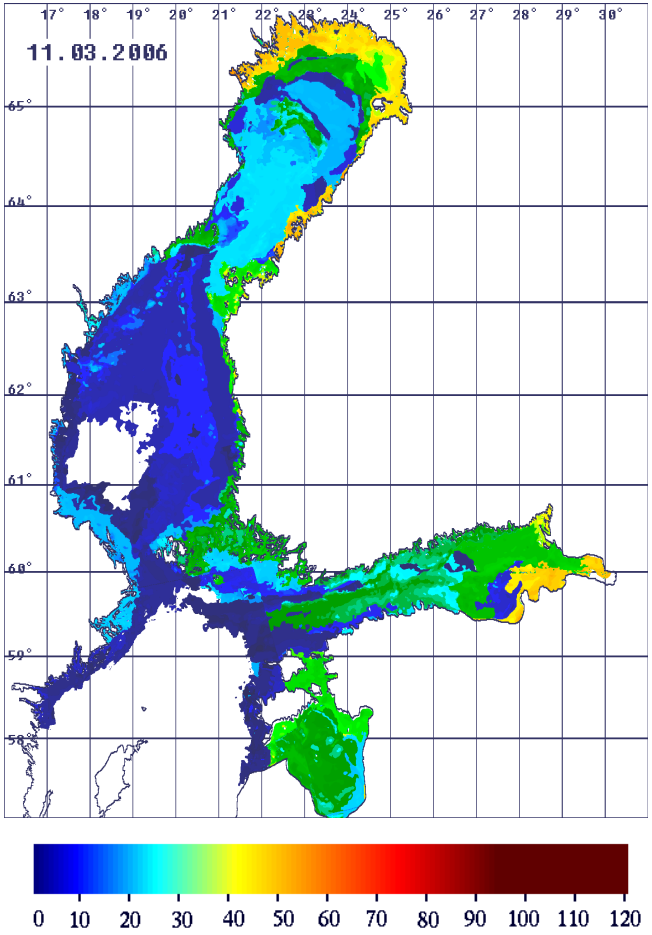

An example of the operational ice thickness chart, March 11 2006.

- One-dimensional thermodynamic snow/ice model, HIGHTSI.
- The model was forced with ECMWF (European Centre for Medium-Range Weather Forecasts) 24 hours forecasts of wind speed, air temperature, relative humidity, cloudiness and precipitation.
- In order to parametrize the ocean heat flux, ice concentrations derived from SAR data using the FIMR open sea algorithm as inputs to HIGHTSI.
- The snow was increased with incoming precipitation and decreased with surface melting and formation of snow-ice and superimposed ice.
- The ice was increased with snow to ice transformation at snow-ice interface and mass balance at the ice-water interface.

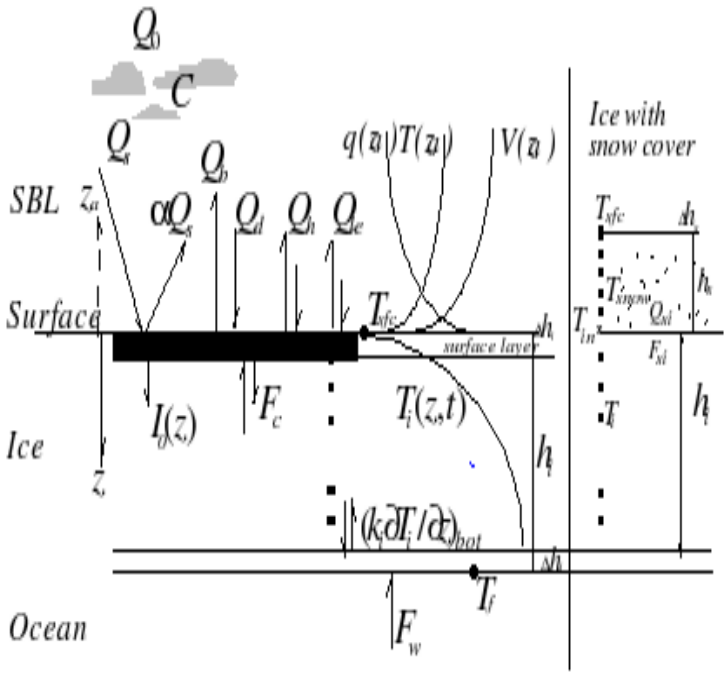

– Q_h, Q_{le}: surface turbulent fluxes of sensible and latent heat

– $I_o(z)$: penetrating solar radiation below surface

– F_c: surface heat conductive flux

– T_{sfc}: surface temperature solved from a surface heat balance equation.

– $T_i(z,t)$ / T_{snow}: vertical temperature distribution within the ice/snow floe solved by a heat conduction equation. The heat flux divergence at ice bottom determines the mass balance

– k_i: heat conductivity of ice

– F_w: the oceanic heat flux assumed to be a function of the ice concentration

– T_f:freezing temperature

– h_s, h_i: snow and ice thickness

– Q_0, Q_s: global downward solar radiation under clear and cloudy sky condition

– C: total cloudiness factor, between 0 and 1

– α: surface albedo

– Q_d, Q_b: downwelling and surface-emitted long wave radiation

- Ice motion detection based on multi-resolution phase-correlation algorithm.
- Fast ice detection by the motion of the ice fields. Fast ice is not moving.
- An incidence angle correction is applied to SAR intensity.
- Segmentation of the SAR images, ice thickness is assigned to each segment.
- The temporal segment-wise median SAR intensity value within four days is used instead of single corrected intensity value. The segment motion, computed based on our ice motion algorithm, is taken into account.

- Feature vector $F_k = [\ H_{hk}\ I_k\ H_{hk}I_k\ 1\ ]$, i.e. terms produced by modulating HIGHTSI ice thickness H_h by the temporal SAR intensity median I ($(a_1 I + b_1)(a_2 H_h + b_2)$).
- The product term $H_{hk}I_k$ is the most significant variable explaining the ice thickness.
- Linear solution:

$$A = F^{\dagger} H \tag{4}$$

F is a feature matrix, the kth line of the matrix contains the feature vector F_k. H contains the ice thickness values from the operational model.
$F^{\dagger}$ is the Moore-Penrose pseudoinverse of F:

$$F^{\dagger} = (F^T F)^{-1} F^T. \tag{5}$$

- Suitable texture measures (segmentwise) can be used instead of SAR intensity (σ^0) in the algorithms. These have been succesfully studied for example over the Caspian Sea.

- Nonlinear method: a two layer Multi-Layer Perceptron (MLP) neural network trained by using the error backprobagation algorithm.
- Feed-forward neural networks, such as MLP, with a single hidden layer of sigmoidal units are capable of approximating uniformly any continuous multivariate function, to any desired degree of accuracy.

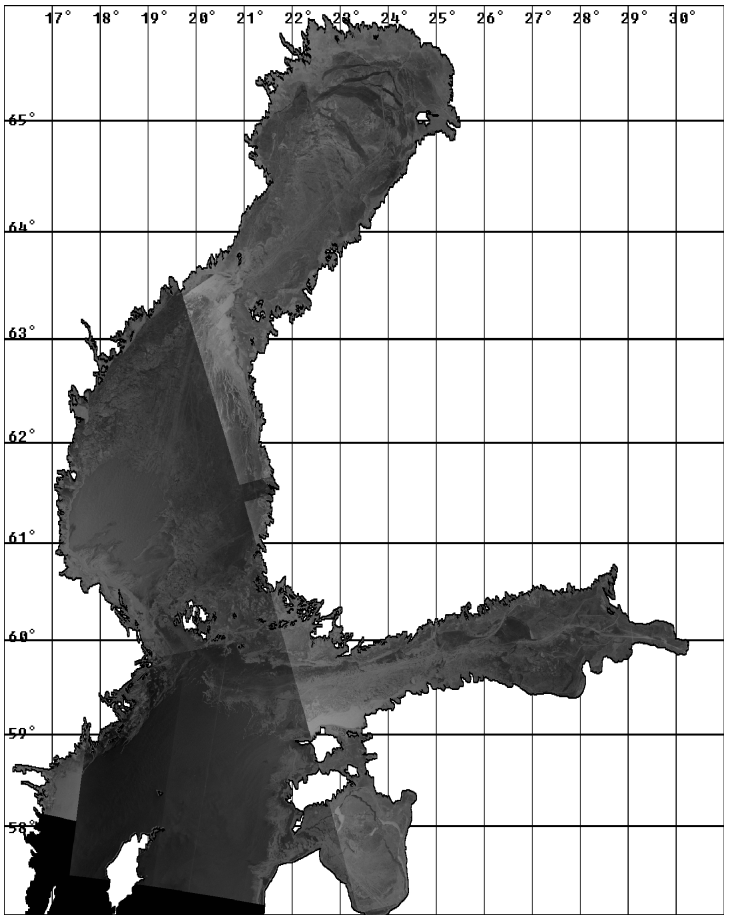

SAR mosaic composed of SAR images acquired before and on March 11th 2006.

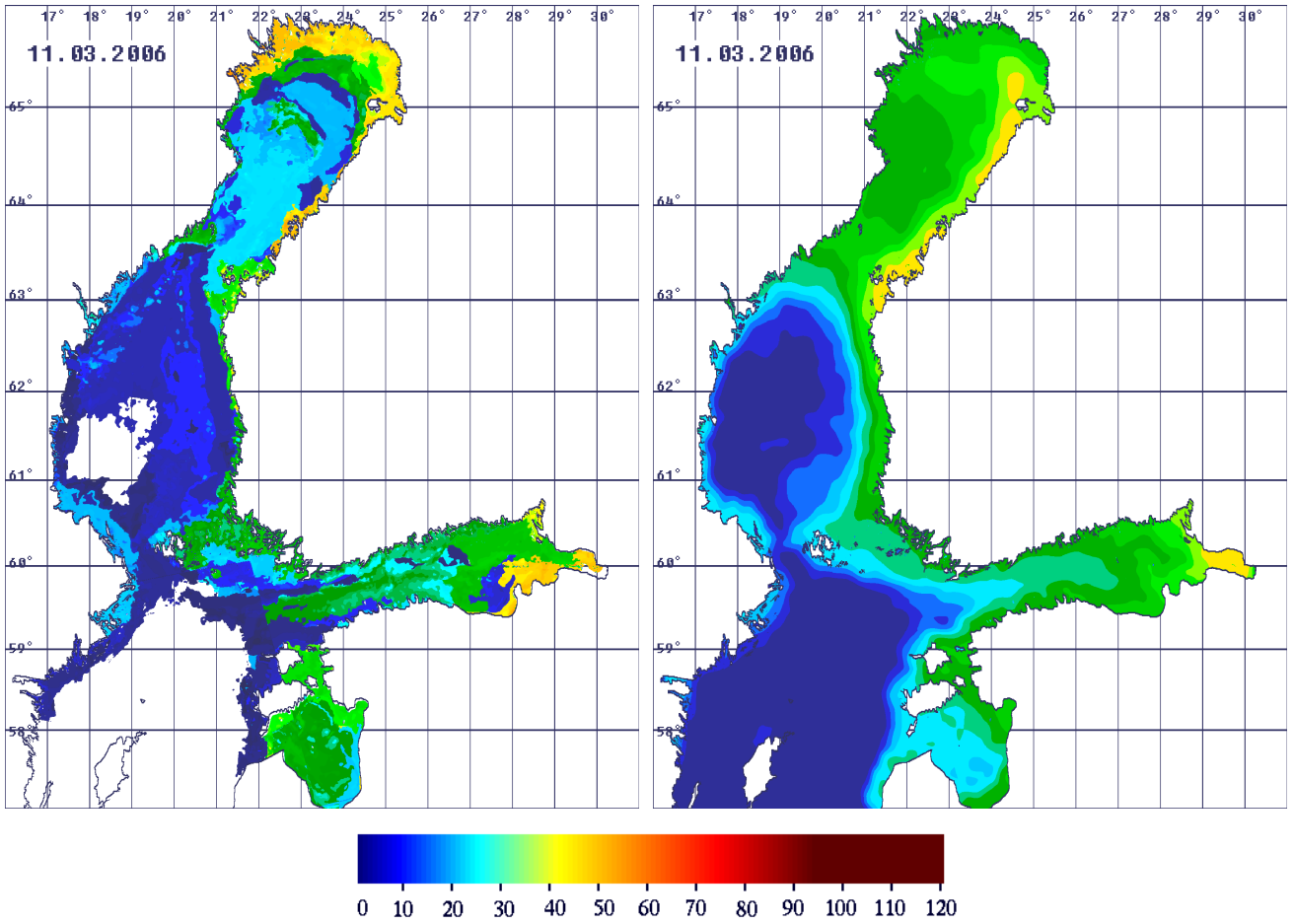

The operational ice thickness chart on March 11th 2006 and the corresponding HIGHTSI ice thickness.

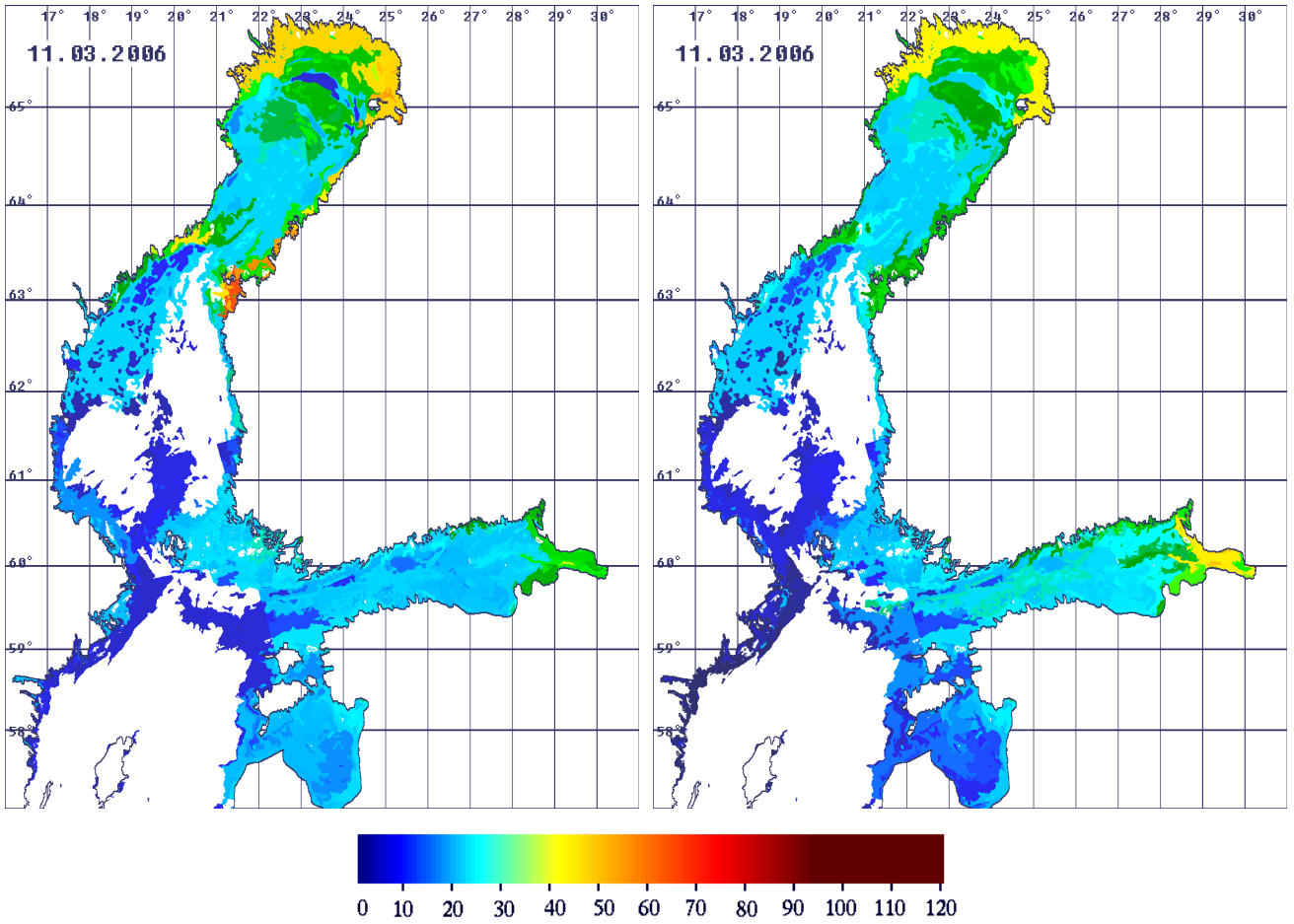

Estimated ice thickness based on the linear algorithm and on the nonlinear algorithm, March 11th 2006.

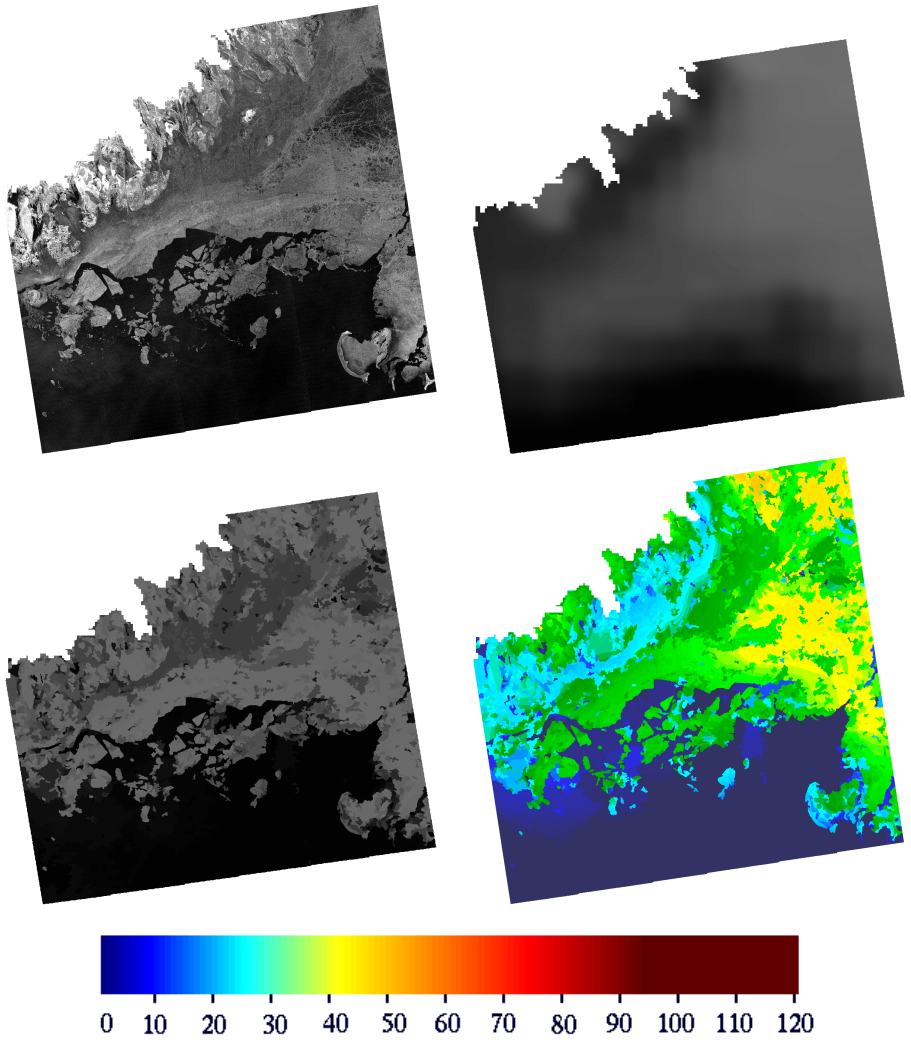

A SAR image of March 23 over the Caspian Sea, the HIGHTSI ice thickness, the segmentwise texture value, and the corresponding ITC.

Segment Shape and Contrast

- Segment related edge features: segment boundary contrast (a simple version: $C = I_{in} - I_{out}$ computed along the segment boundary), and segment features based on a segment bounding polygon with N=20 points or polygon corners.

An example of two artificial segments and their bounding 20-point polygons.

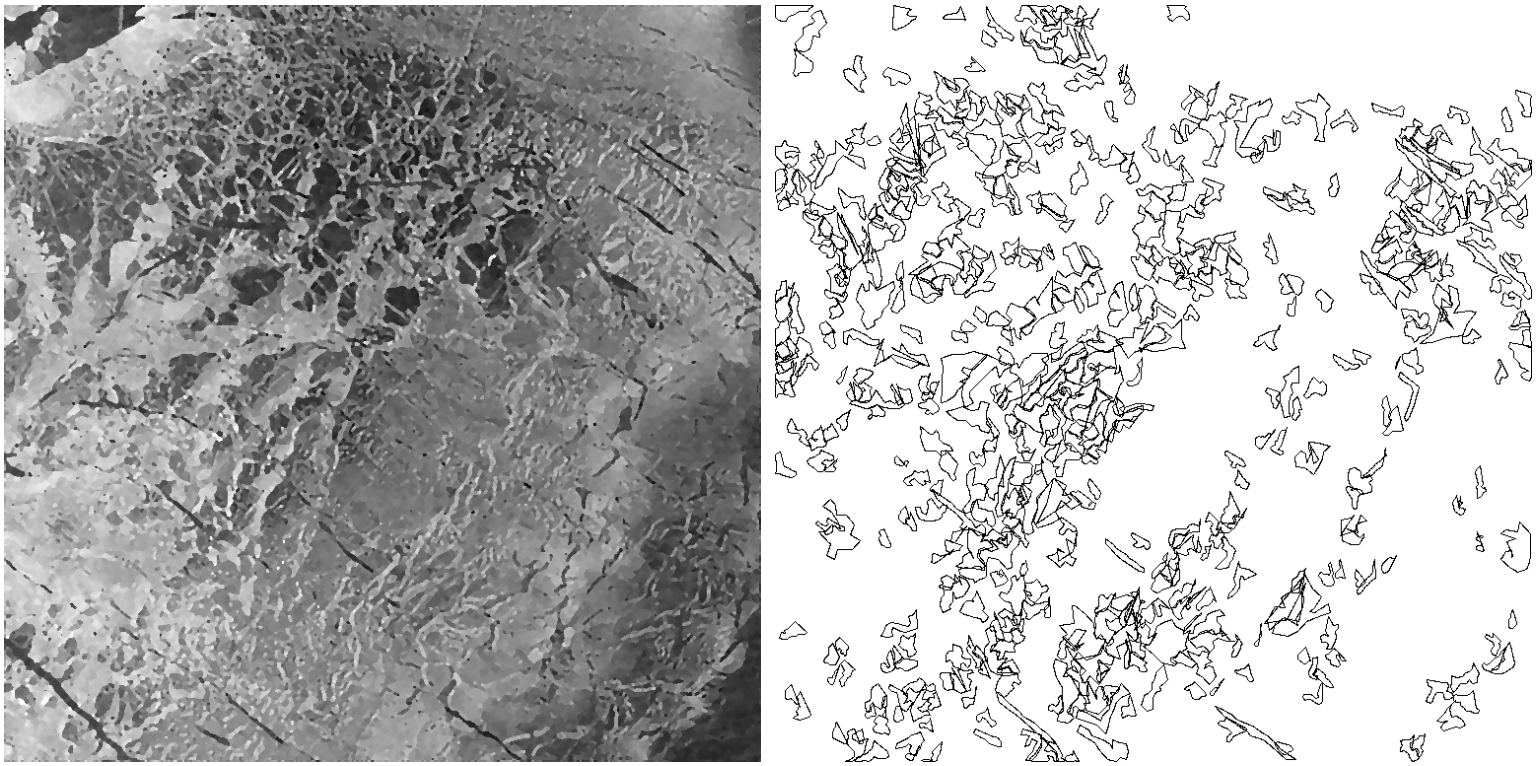

Part of a filtered SAR image, and the edge polygons for the segments within predefined size limits.

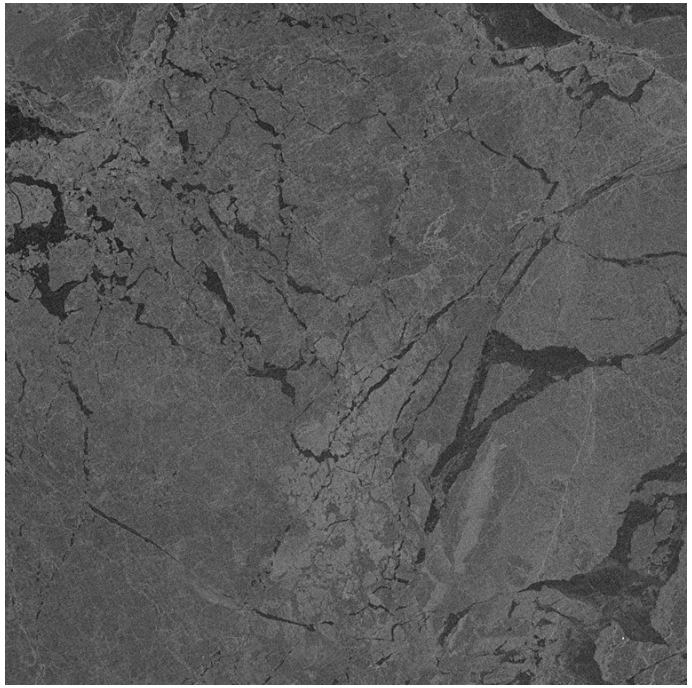

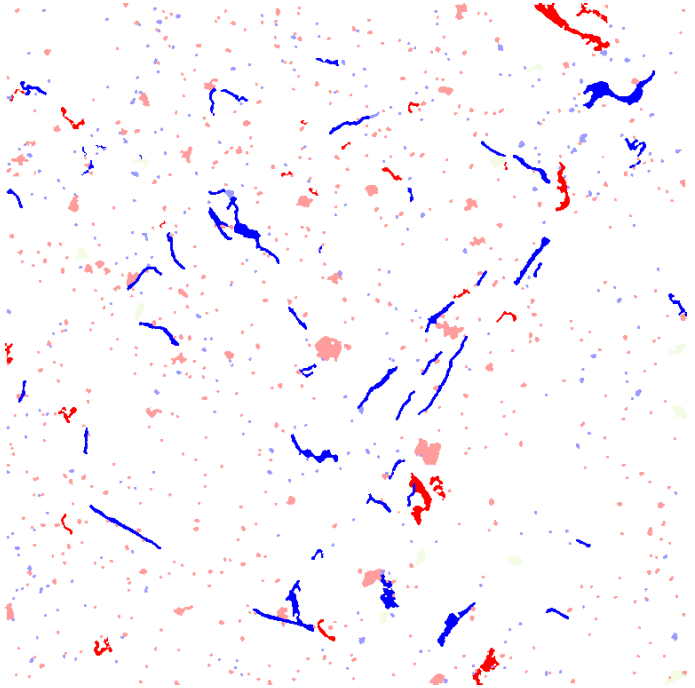

A part of a Radarsat-1 SAR image (Baltic Sea, $\approx 75x75km$), and the the classified features (for segments smaller than a threshold, i.e $A < T_A$). The red segments have the edge contrast $C > T_{ctr2}$ and the blue segments $C < T_{ctr1}$, the segments drawn with brighter red and blue are classified based on the small segment algorithm.

ILMATIETEEN LAITOS
METEOROLOGISKA INSTITUTET
FINNISH METEOROLOGICAL INSTITUTE

SAR Feature Extraction and Template Matching Approaches

- These methods try to locate 2-D elementary features from SAR data.
- Such features are computed for areas called data windows here.
- Sea ice SAR images contain structures consisting of different types of edges.
- These elementary features can be extracted based on several techniques.
- The basic idea is to extract data windows (square or round-shaped) from SAR with some interesting features, and use an iterative algorithm to capture these features into a set of elementary features. This set can then be used in classification of the SAR data.
- The elementary features have the same size and shape as the SAR data windows.

- One simple measure of similarity between a SAR and an elentary feature vector is:

$$D(w_i, x) = \cos(\gamma) = \frac{w_i \cdot x}{|w_i||x|}. \quad (6)$$

- To take into account the rotations, either multiple rotated versions of each elementary vector can be used, or the matching can be performed in polar coordinates.
- As these features have a larger support than just one pixel, the classification is less sensitive to speckle than using pixel-wise σ^0 data.

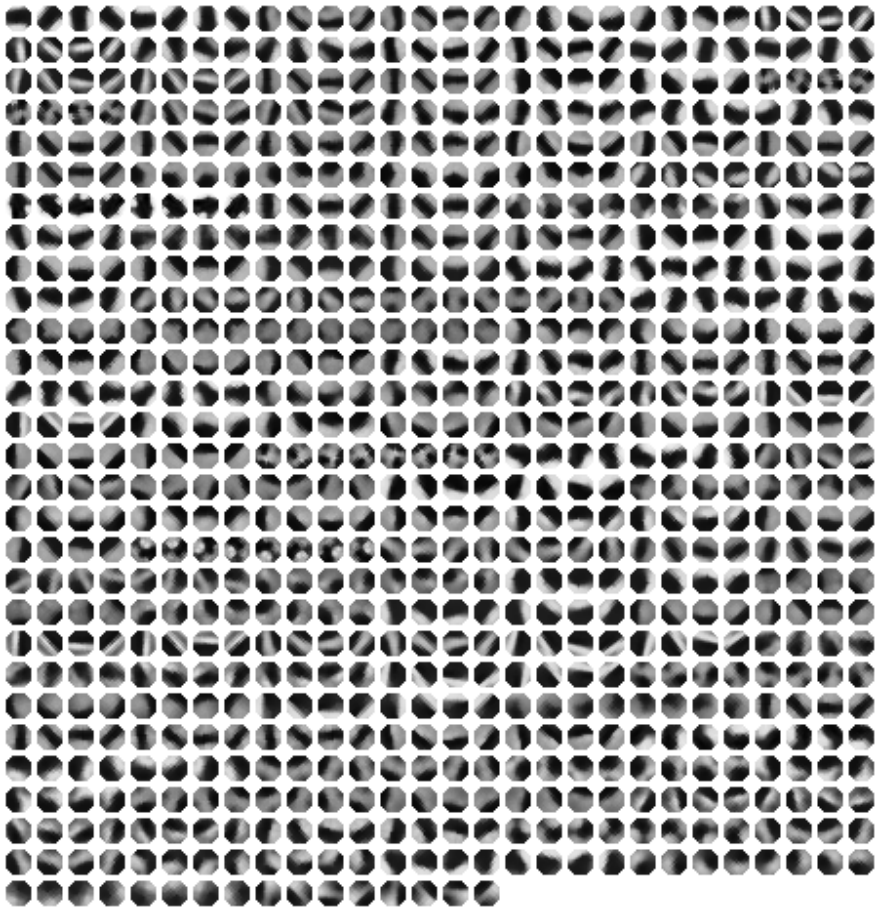

An example of an elementary vector set with all the vectors rotated in steps of 45 degrees.

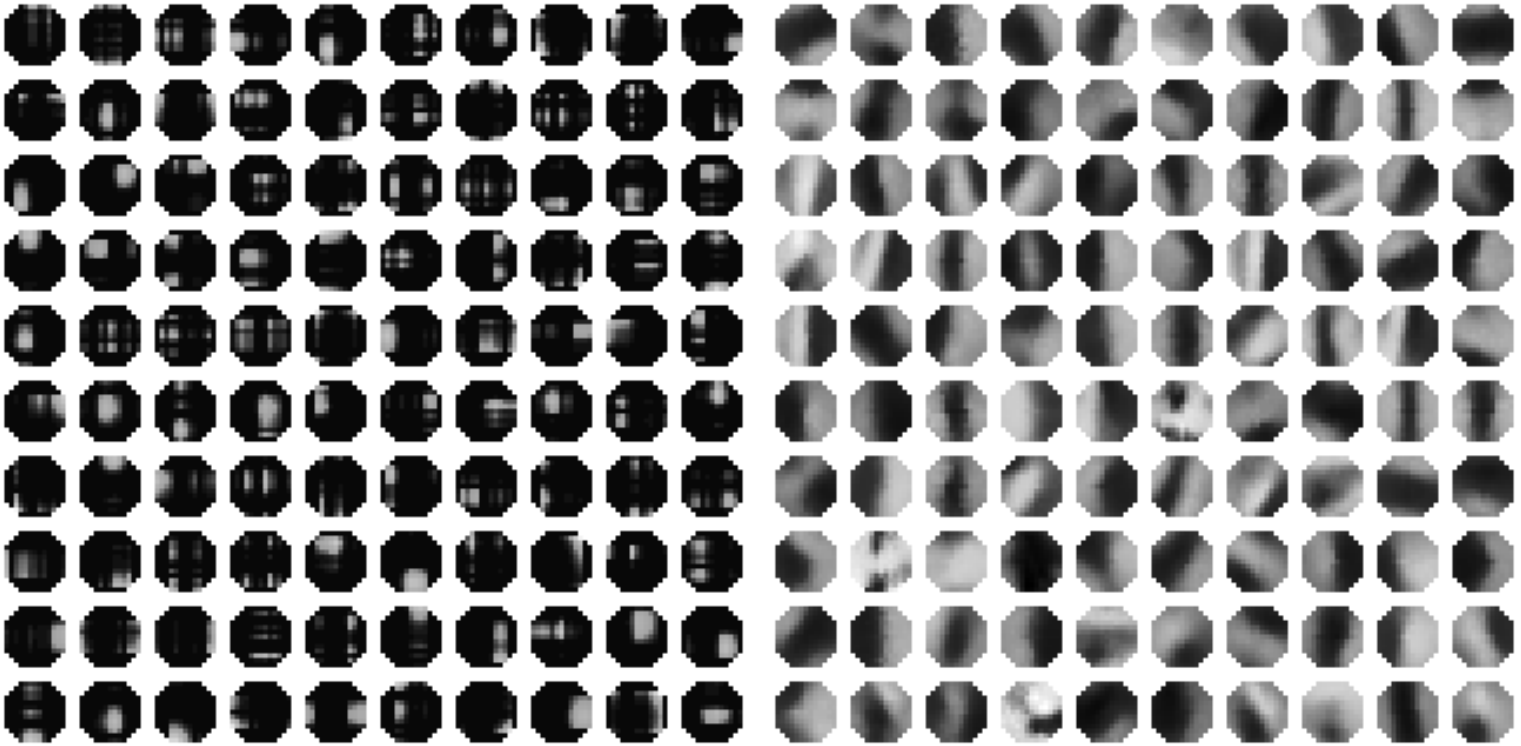

A set of SAR basis vectors produced by NTF (left), and a set of

SAR elementary features produced by cluster reconstruction (right). The features B_c are produced based on clustering of the weights W of the basis vectors B and then produced as $B_c = W_c B$

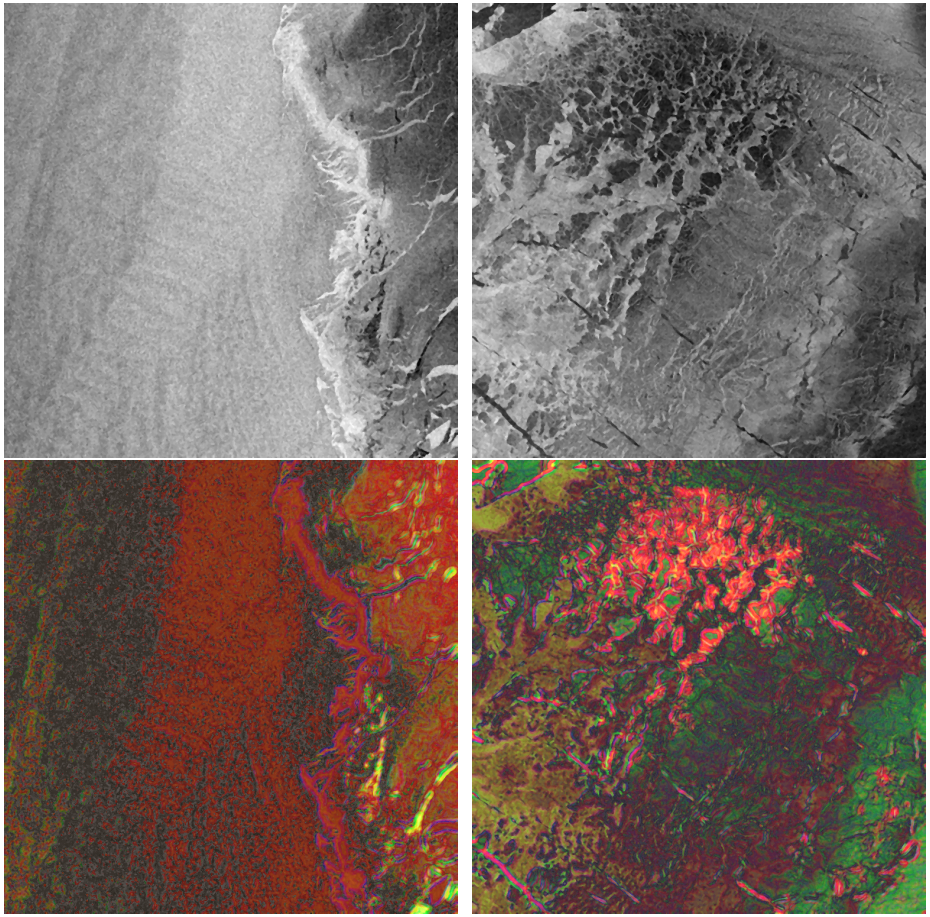

Two SAR image windows and visualizations of their NTF feature classifications.

Multimtemporal SAR Analysis - Ice Drift

- Phase correlation algorithm: 2-D FFT is applied to the data window, the FFT-coefficients of the two image windows are normalized by their magnitudes, then the FFT-coefficients of the two image windows are multiplied and the inverse 2-D FFT is applied (I_p is the phase correlation image computed from the the normalized cross power spectrum):

$$\begin{aligned}(dx, dy) &= \mathrm{argmax}_{(x,y)} \{I_p(x, y)\} \\ &= \mathrm{argmax}_{(x,y)} \left\{ FFT^{-1} \left(\frac{({X_1}^*(k,l) X_2(k,l))}{|{X_1}^*(k,l) X_2(k,l)|} \right) \right\},\end{aligned} \tag{7}$$

- Because the FFT assumes that the data is periodic, a Gaussian window is applied to the data windows before the transformation.
- The best matching displacement is then defined by the maximum of the phase correlation.

- The search for the best local phase correlation is performed in two resolutions: coarse and fine resolution.
- Vector median filtering is performed with a given radius R_m. The radius depends on the local phase correlation magnitude.

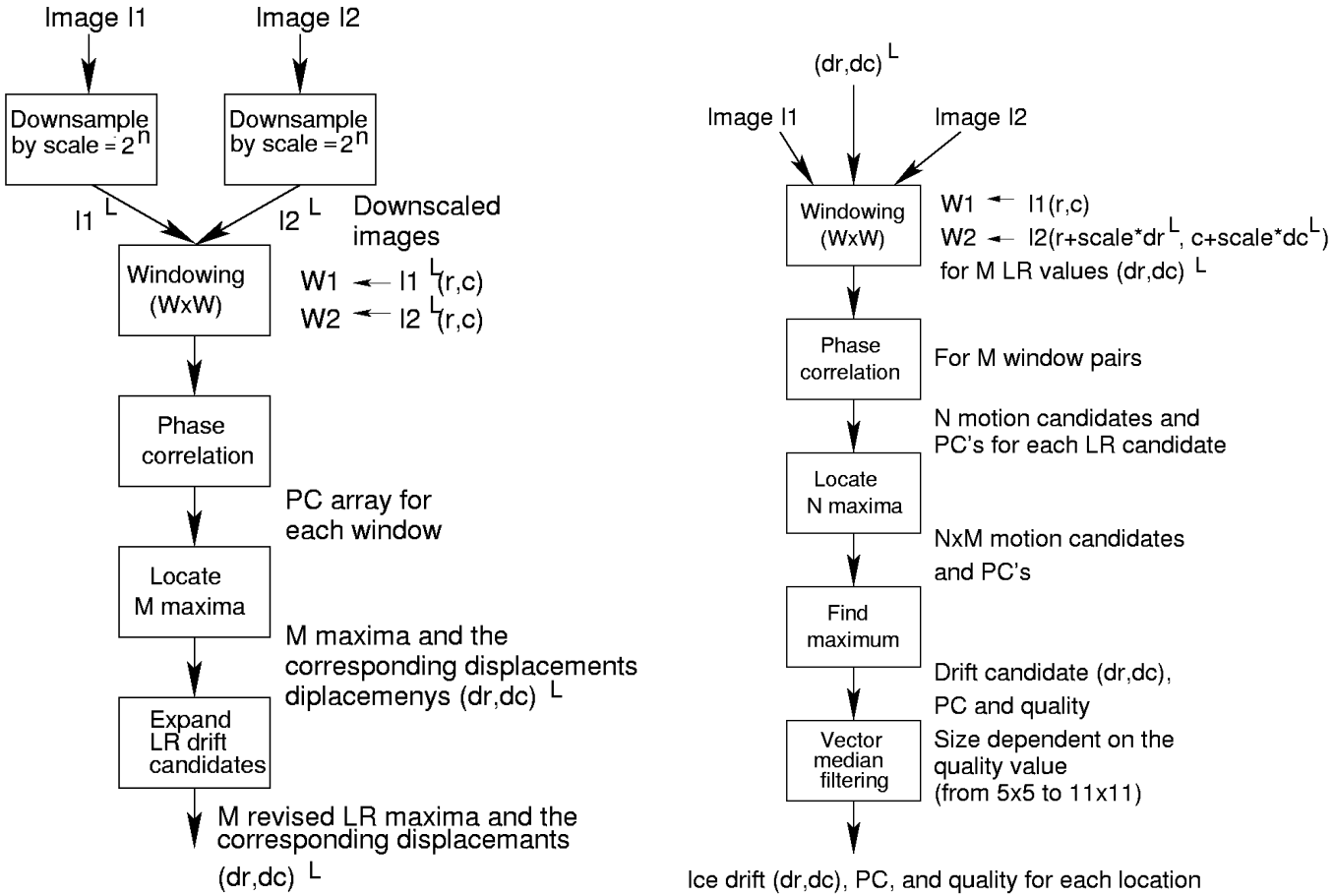

Block diagram of the ice drift algorithm low resolution part (left), and high resolution part (right), (Karvonen, OS, 2012).

- Suggested quality measures:
  - $Q_1 = PC_1(1 - \sum_{k=2}^{n} \frac{PC_k}{PC_1} D_k) = PC_1 - \sum_{k=2}^{n} PC_k D_k$
  - $Q_2 = 1 - \sum_{k=2}^{n} \frac{PC_k}{PC_1} D_k$
  - $Q_3 = PC_1 - PC_2$
  - $Q_4 = PC1 \times (PC_1 - PC_2)$
  - $Q_5 = PC_1/N_p$
  - $Q_6 = 1.0 - (PC_2/PC_1) = \frac{PC_1 - PC_2}{PC_1}$

- Quantities derived from the ice drift vector field F:
  - Divergence: $D(F) = \nabla \cdot F$
  - Curl: $C(F) = \nabla \times F$
  - Shear: $S(F) = \sqrt{\left(\frac{\partial dc}{\partial c} - \frac{\partial dr}{\partial r}\right)^2 + \left(\frac{\partial dc}{\partial r} - \frac{\partial dr}{\partial c}\right)^2}$
  - Total deformation: $D_T(F) = \sqrt{S^2 + D^2}$
- Discrete estimates straightforward to compute based on differences, e.g. $D(F) = \frac{1}{2}[dr(i+1,j) - dr(i-1,j) + dc(i,j+1) - dc(i,j-1)]$

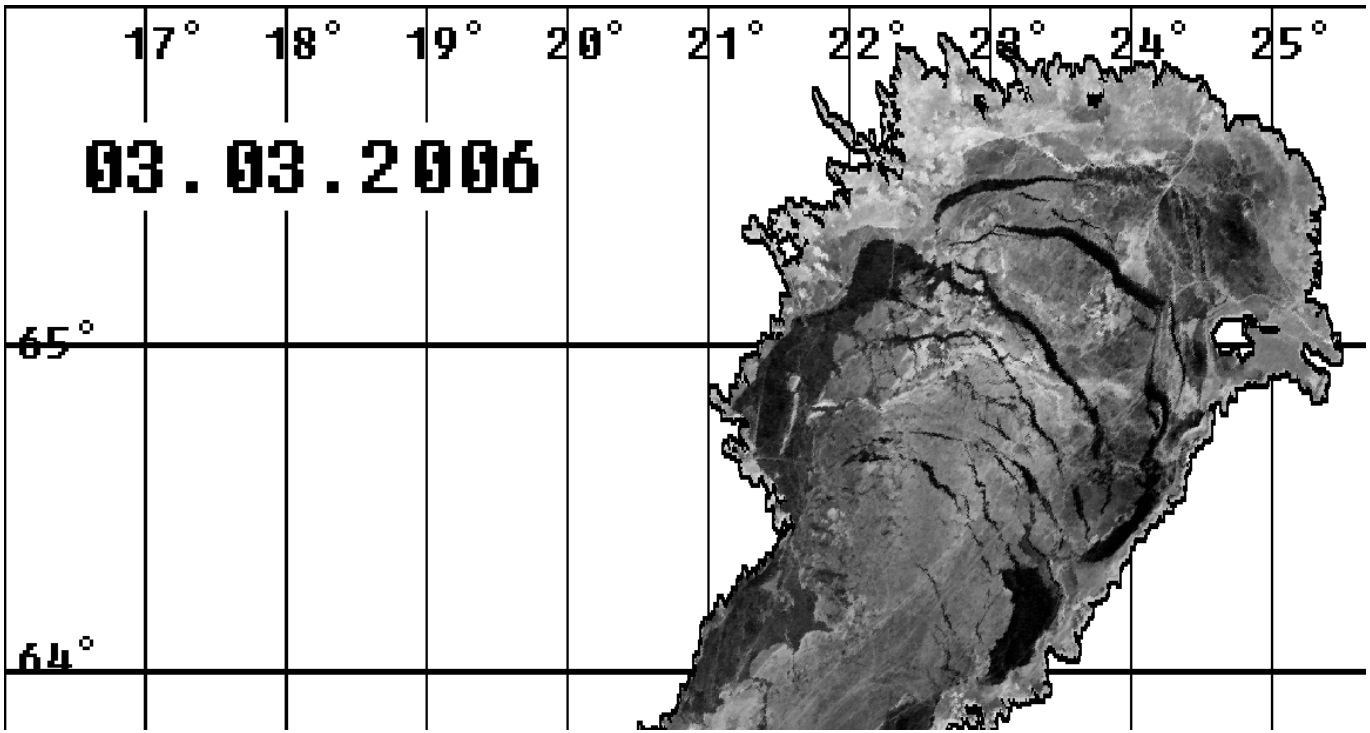

SAR March 3rd 2006, Bay of Bothnia.

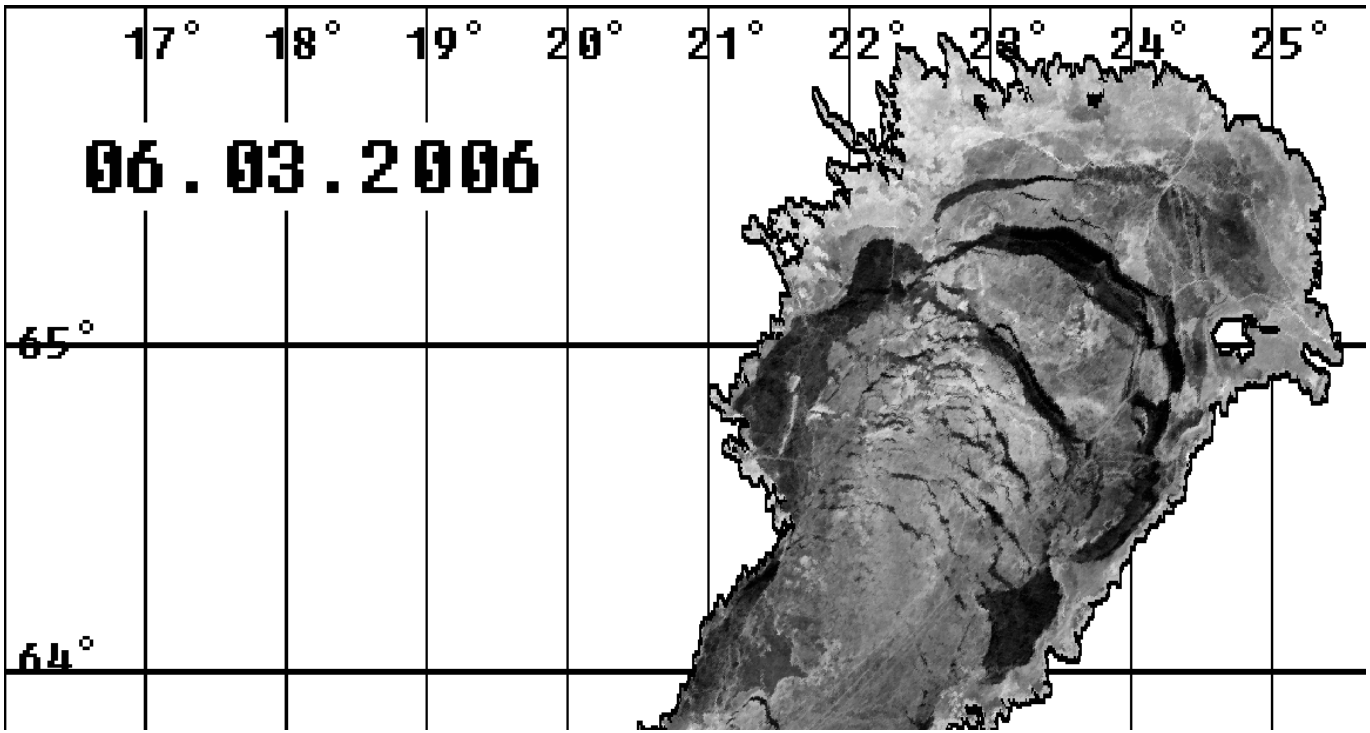

SAR March 6th 2006, Bay of Bothnia.

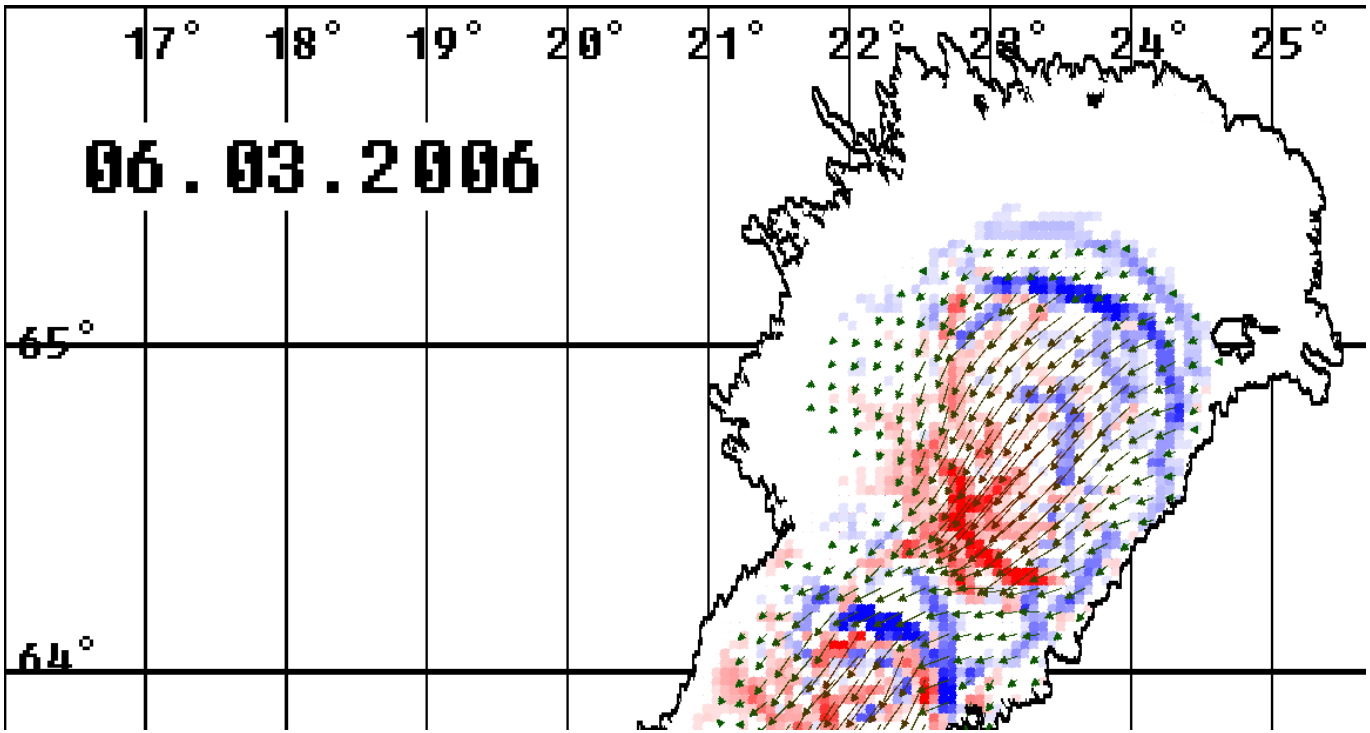

Estimated motion between the two SAR images in the previous figures.

- Comparison to buoy motion in the Bothnian Bay drift ice field. GPS signal time resolution is about 1 hour.
- Temporally closest buoy location to the SAR acquisition used in the comparison.
- 32 buoy motion vectors corresponding to 32 SAR image pairs during the time period March 11th $\rightarrow$ April 19th 2005.

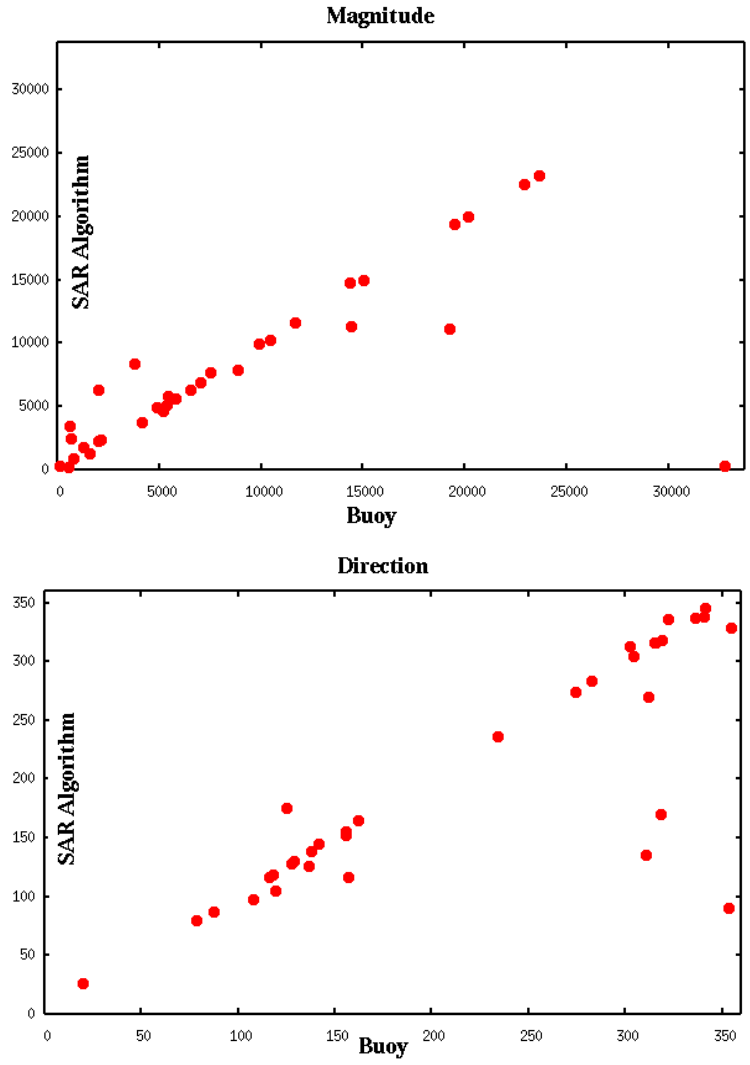

Buoy motion vs. SAR motion, magnitude (meters) and direction (degrees).

- Coefficient of determination, R^2
  Magnitude: $R^2 = 0.452$
  Direction: $R^2 = 0.641$
- Maximum allowed time difference between a SAR image pair in this validation was 4 days.

ILMATIETEEN LAITOS
METEOROLOGISKA INSTITUTET
FINNISH METEOROLOGICAL INSTITUTE

Multitemporal SAR Analysis - Fast Ice

- Fast ice is the ice which does not drift, attached to land (land fast ice).
- Fast ice can be detected by thresholding the ice motion, i.e. finding the ice areas which have not been moving for a given time period, e.g. two weeks.
- Also algorithms locating the ice areas adjacent to land work pretty well.

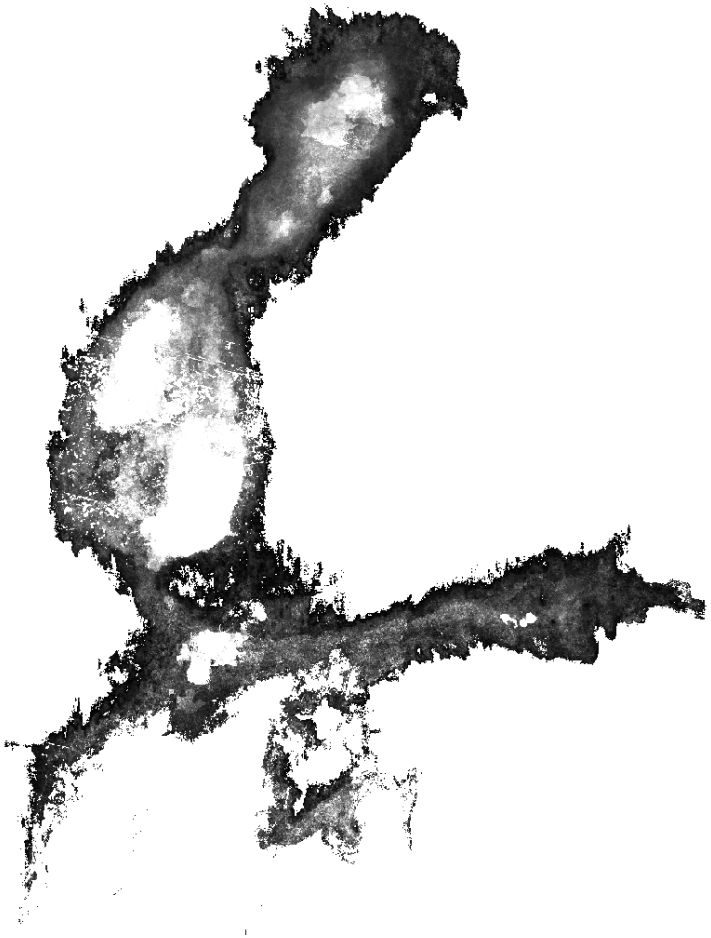

Mean ice motion magnitude for two weeks before March 5th 2010. Bright tones represent larger motion. The fast ice areas can be derived from this data.

- Another way to locate fast ice fields is to use the temporal cross-correlation between image mosaics (or image pairs).
- The cross-correlation is computed for window, with a suitable size (defined by the radius R), around each mosaic pixel (grid cell).
- The temporal CC minimum, within e.g. 1-2 weeks, is then found for each grid cell.
- The fast ice zone can be located by thresholding the temporal CC minimum grid.

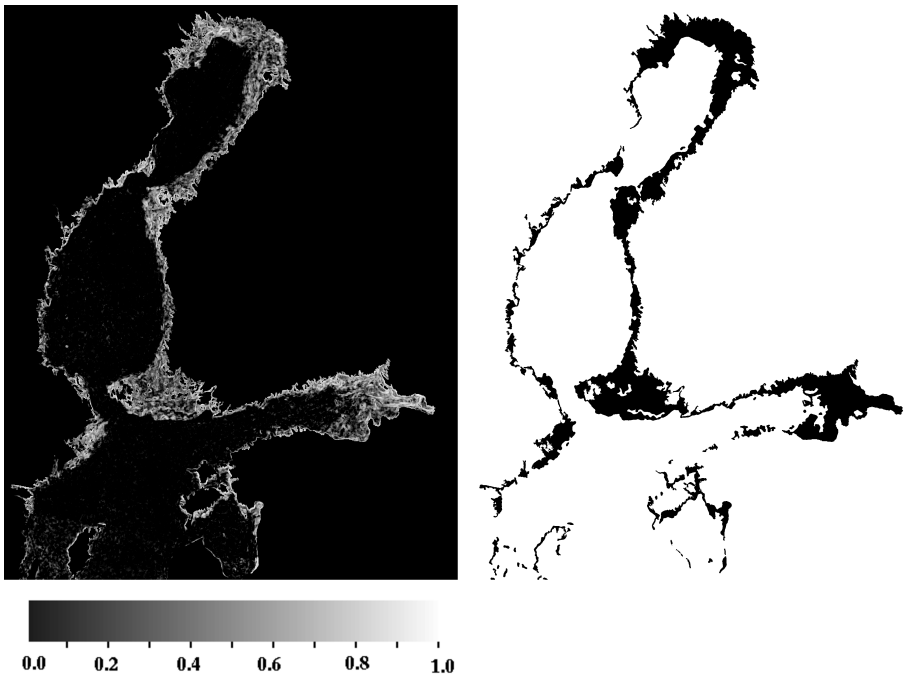

The one-week cross-correlation minimum for the Baltic Sea SAR mosaics (a). The cross-correlation is computed between SAR mosaics of two adjacent days. At each pixel location the minimum of the cross-correlation during the one week period is shown. The fast ice mask produced based on thresholding of the cross-correlation minimum (b).

Identification of Deformed Ice

- Different methods can be applied. The simpliest method is to find high backscatter areas in the incidence angle images. The highly deformed areas can better be located in HV data.
- Edge detection in combination with the high backscatter.
- Signal to noise ratio (local mean divided by local standard deviation) or ENL.
- Gradient-based features.
- Feature detection, e.g. using feature templates derived from SAR data.
- Segment property analysis after segmentation (shape, contrast to background, ...)
- HV channel data to detect the highly deformed areas (they can not be distinguished at HH chanel), at HV channel these areas have a higher backscattering.
- Multitemporal analysis: deformation occurring in the diverging ice areas.

Coastal and Ship Radars

- Marine radars operate at 10 GHz ($\lambda \approx 3$cm) and 3 GHz ($\lambda \approx 10$ cm), i.e. at X and S bands.
- Bearing (azimuth or angular) resolution: the ability of a radar system to separate objects at the same range, but at slightly different bearings. The degree of bearing resolution depends on radar beamwidth and the range of the targets.
- Range resolution: the ability of a radar system to distinguish between two or more targets on the same bearing but at different ranges. Depends on the radar pulse length.
- Radar video server developed by a Finnish company Image Soft Oy.
- 20 MHz sampling rate.
- Based on PC technology, forms PPI (Plan Position Indicator) images from the radar signal, the triggering pulse and the antenna pulse.
- PPI is the most common type of radar display. The radar antenna is usually represented in the center of the display, so the distance from it and height above ground can be drawn as concentric circles.
- Imaged area: 40 km by 40 km, image size 1200x1200 pixels, nominal resolution $\approx$ 33 m.
- Radar images require preprocessing: temporal median in the beginning of each minute (15-20 sec).

- After temporal median filtering the data is transmitted via a cellular phone network modem to an FMI server every two minutes (the temporal sampling is limited by the modem bandwidth).
- The transmission is automatically monitored, and a message to the maintaining persons if automatically sent if there is a break in delivery.
- On the FMI server the images are normalized to reduce the effect of the distance attenuation to the radar response.
- Operational radar images with 15 minute interval (at the moment for FMI internal use).
- The ice drift is computed for image pairs with a 10 minute temporal spacing, and also delivered operationally (as a vector field image).
- Studies of tracking automatically selected ice objects in time have been made. In this study the methodology has been tested and its poentials evaluated. The tracking experiments have been made with 10 minute interval.

- Homomorphic filtering has its background in optical images processing.
- Image intensity for an optical is presented as a product of the illumination L and reflectance R (R is a property describing the scene objects, L results from the lighting conditions): $I(r, c) = L(r, c)R(r, c)$
- In homomorphic filtering, a log transform is first applied to make the components additive.
- Then a high pass filter is applied. This assumes that the lighting condition is assumed to vary slowly across the image and reflectance is changing faster (sharp object edges).

Homomorphic Filtering

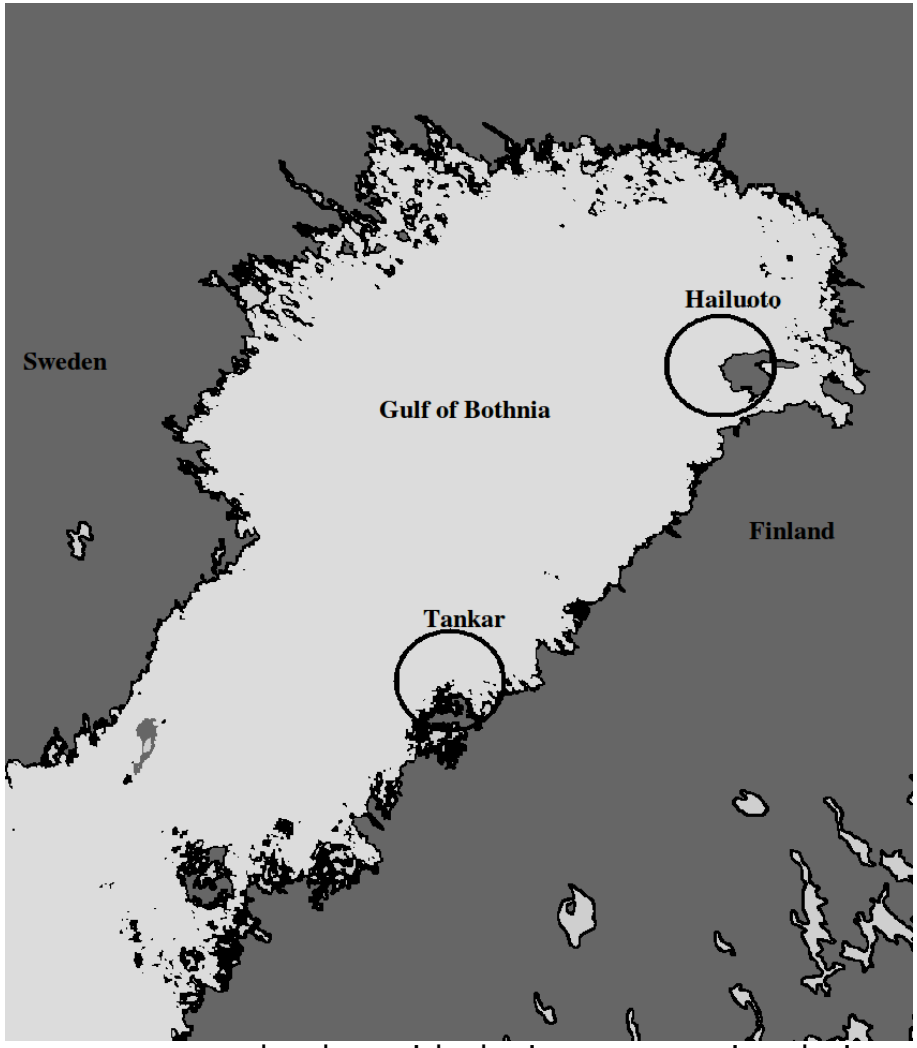

Locations of the current coastal radars with the image capturing device and their range.

A radar image, Feb 25, 2011, 06:50 UTC.

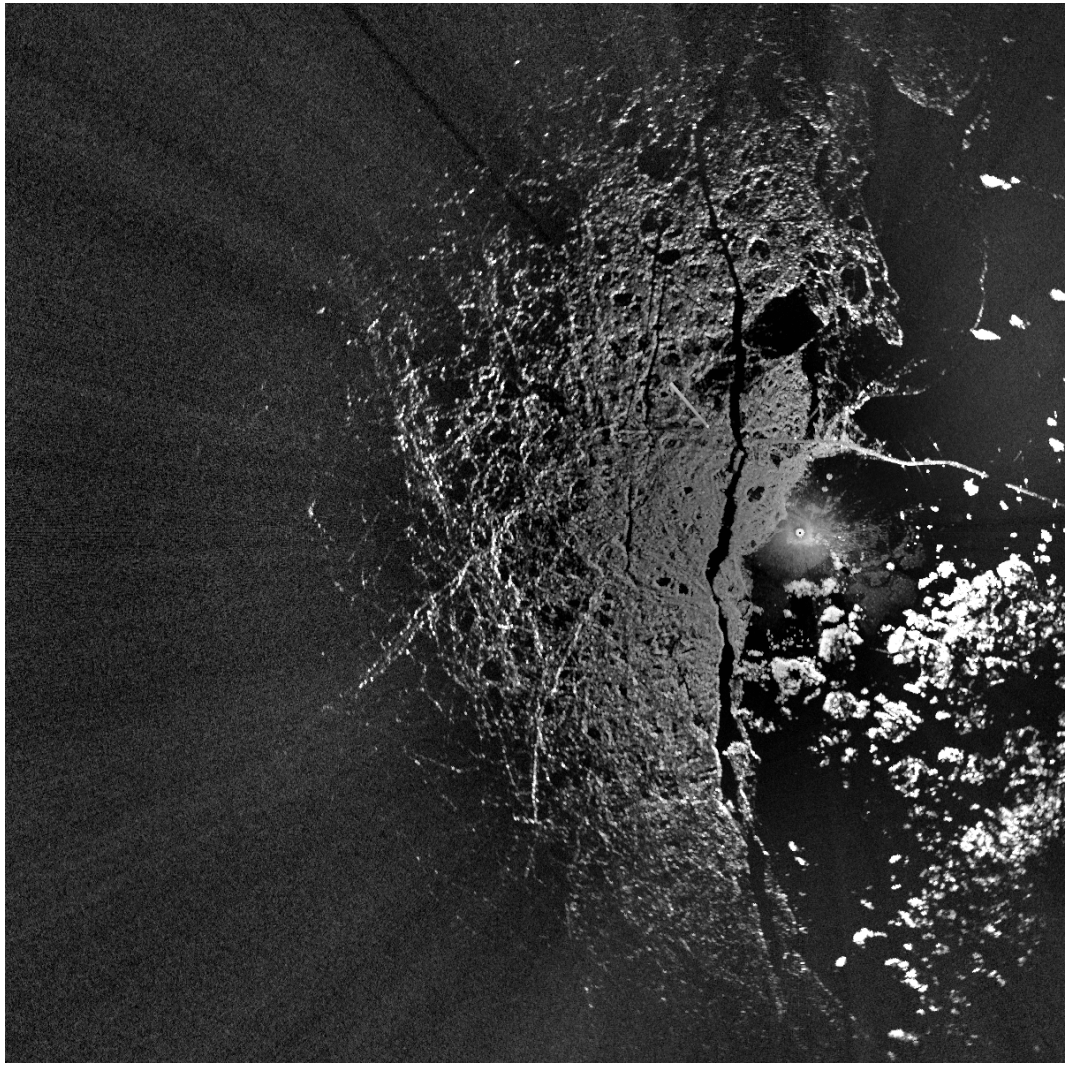

The radar image after distance normalization.

Tracking Algorithm

- Selection of objects
  - In a given grid locate the local maximum of E(r,c,R):

$$E(r, c, R) = \sigma(r, c, R) N_c(r, c, R) N_e(r, c, R) \tag{8}$$

  $\sigma(r, c, R)$ is the local standard pixel value deviation within a radius R from the location (r,c), $N_c(r, c, R)$ is the number of detected corner points within the same radius, and $N_e(r, c, R)$ number of detected edge points within the same radius.
  - These objects contain corners, edges and have a good contrast.
- Feature tracking
  - For each object locate the phase correlation (PC) maximum in two (coarse and fine) resolutions between each pair of radar images:

$$\begin{aligned}(dx, dy) &= \text{argmax}_{(x,y)} \{PC(x, y)\} \\ &= \text{argmax}_{(x,y)} \left\{ FFT^{-1} \left(\frac{(X_1{}^*(k,l) X_2(k,l))}{|X_1{}^*(k,l) X_2(k,l)|} \right) \right\},\end{aligned} \tag{9}$$

- Also normalized cross-correlation (CC) can optionally be used:

$$(dx, dy) = \text{argmax}_{(x,y)} CC(x, y), \tag{10}$$

CC can be computed either in Fourier domain (after normalizing the inputs by subtracting the means and dividing by the standard deviations) or directly:

$$CC(x, y) = \frac{1}{N} \sum_{i=1}^{N} \sum_{j=1}^{N} \frac{(x_1(i, j) - \mu_1)(x_2(i - x, j - y) - \mu_2)}{\sigma_1 \sigma_2} \tag{11}$$

- For each object between two radar images: In coarse resolution M motion candidates corresponding to M highest PC values are found. In the fine resolution, the maximum among the coarse resolution motion candidates is selected as the final fine scale motion.

- Rotation is taken into account by including slightly rotated versions of another (the first because the feature is centered in it) of the image objects pairs (from -15 to 15 degrees).

- A simple quality measure Q:

$$Q = PC_{max}/N_p, \tag{12}$$

  For one image window pair PC_{max} is the maximum phase correlation, N_p is the number of phase correlation values exceeding a threshold T dependent on PC_{max} (e.g. $T = 0.7PC_{max}$.
- Quality threshold $T_q = 0.05$. The object is "lost" after $Q < T_q$.
- Q rapidly decreases as ice begins to move.
- Q for moving ice decreases as the distance from the origin increases.

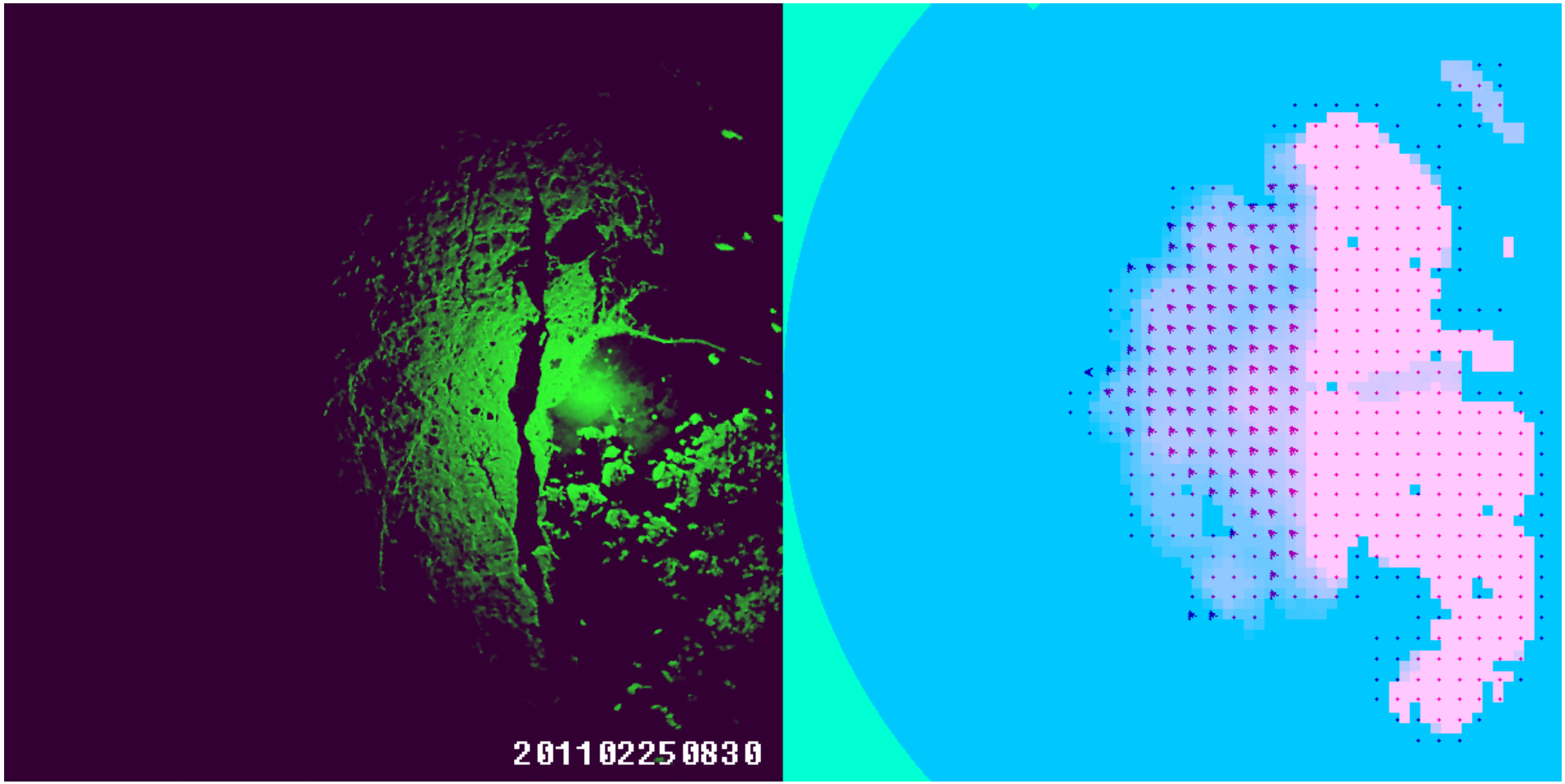

Radar image (Tankar, Feb 25, 2011, 08:30) and ice drift vector field derived from multitemporal analysis.

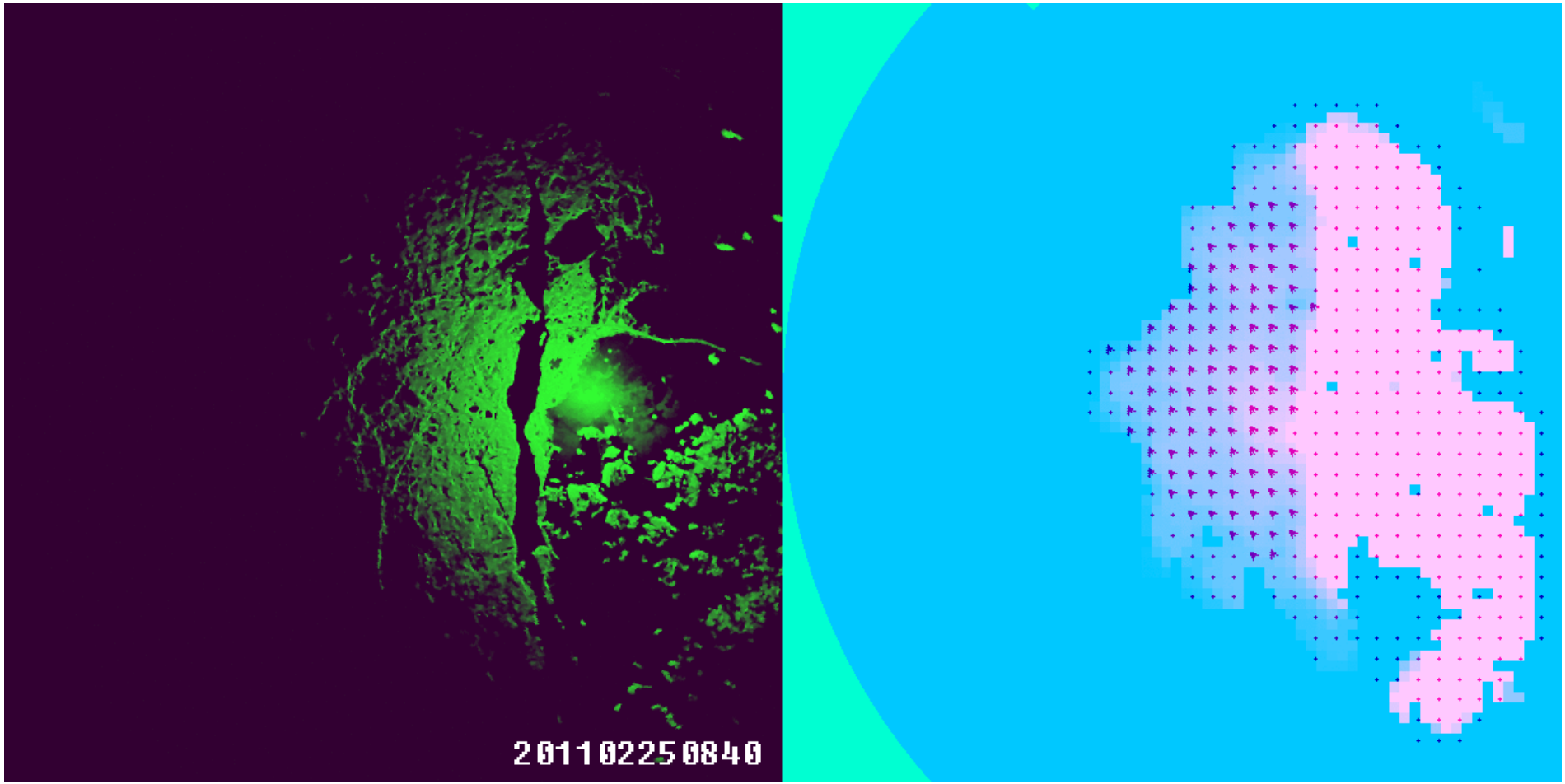

Radar image (Tankar, Feb 25, 2011, 08:40) and ice drift vector field derived from multitemporal analysis.

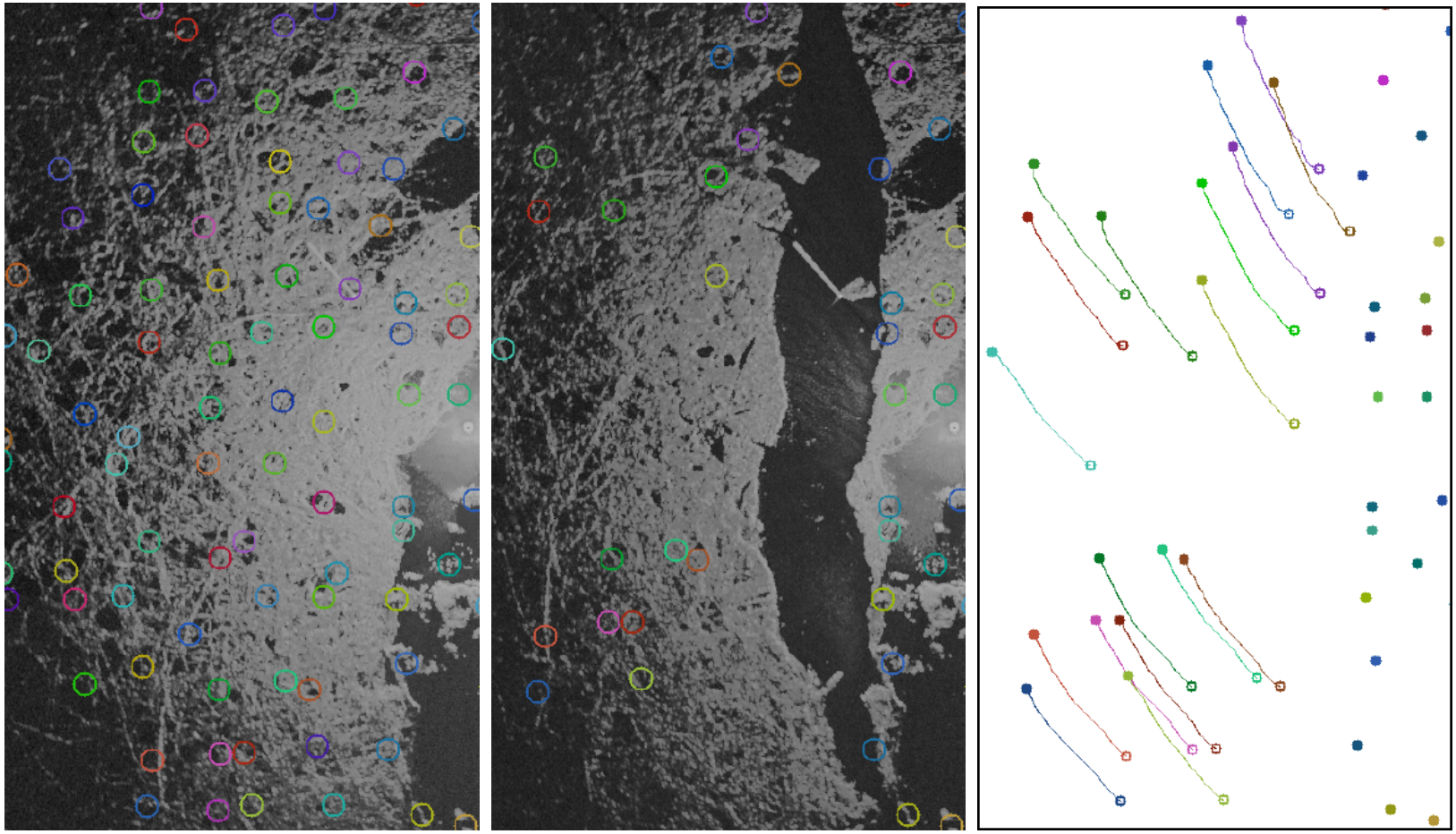

Tracking case, Feb 25, 2011, 12 hours.

Derived Quantities

- Divergence of a vector field F

$$D(F) = \nabla \cdot F.$$

  dr and dc are the motion in row and column directions.

- Curl of a vector field F

$$C(F) = \nabla \times F.$$

- Shear for a vector field F

$$S(F) = \sqrt{\left(\frac{\partial dc}{\partial c} - \frac{\partial dr}{\partial r}\right)^2 + \left(\frac{\partial dc}{\partial r} - \frac{\partial dr}{\partial c}\right)^2}.$$

- Total deformation

$$D_T(F) = \sqrt{S^2 + D^2}.$$

- Can be estimated (discrete estimates) based on the neighboring buoy motions.
- Average ice velocity.

Conclusion

- The major ice parameters can be estimated based on EO.
- From SAR alone most parameters can be estimated, these parameters are ice deformation, ice concentration, ice drift (multitemporal analysis).
- Quantitative SAR-based ice thickness estimation requires additional information, qualitative estimates possible from SAR.
- Dual-polarized (HH/HV) SAR data improves the estimation of the ice parameters.
- Fully polarimetric data has not been widely utilized in operational SAR-based sea ice monitoring yet, because no wide swath mode fully polarimetric data is available and will not be available in the near future.
- HOWEVER, RISAT (operational) and Radarsat constellation (2018) have the so-called compact polarimetry mode, which gives similar results as full polarimetry (and is lighter to implement).
- Radiometer (e.g. AMSR-2) can be used for coarse scale ice concentration estimation. Coarse resolution is a problem in coastal and archipelago areas.
- Radiometer (e.g. AMSR-2) or VIS/IR (MODIS) data can be used to improve detection of thin ice. Cloud cover is a problem with the VIS/IR data.

- Validation is a real problem: e.g. ice thickness can vary a lot within a single EO instrument pixel (e.g. within a 100m SAR pixel), and a lot of point measurements are required to get reliable statistics.
- Validation using other EO instruments or e.g. EM measurement lines. Extensive validation still too expensive.
- Space-borne altimeters data only gives qualitative IT information, accuracy too coarse for pointwise ice thickness estimation for navigation purposes.

Thank You!